

USARIEM TECHNICAL REPORT T0-01-xx

**EVALUATION AND REFINEMENT OF THE ENVIRONMENTAL STRESS INDEX (ESI)
FOR DIFFERENT CLIMATIC CONDITIONS AND DISTANCES BELOW AND ABOVE
SEA LEVEL**

Daniel S. Moran, Ph.D.

Kent B. Pandolf, Ph.D.

Richard R. Gonzalez, Ph.D.

Biophysics and Biomedical Modeling Division

November 2001

DISTRIBUTION STATEMENT A

Approved for Public Release

Distribution Unlimited

20011120 050

U.S. Army Research Institute of Environmental Research

Natick, MA 01760-5007

REPORT DOCUMENTATION PAGE			Form Approved OMB No. 0704-0188	
Public reporting burden for this collection of information is estimated to average 1 hour per response, including the time for reviewing instructions, searching existing data sources, gathering and maintaining the data needed, and completing and reviewing the collection of information. Send comments regarding this burden estimate or any other aspect of this collection of information, including suggestions for reducing this burden, to Washington Headquarters Services, Directorate for Information Operations and Reports, 1215 Jefferson Davis Highway, Suite 1204, Arlington, VA 22202-4302, and to the Office of Management and Budget, Paperwork Reduction Project (0704-0188), Washington, DC 20503.				
1. AGENCY USE ONLY (Leave blank)		2. REPORT DATE November 2001		3. REPORT TYPE AND DATES COVERED TECHNICAL REPORT
4. TITLE AND SUBTITLE EVALUATION AND REFINEMENT OF THE ENVIRONMENTAL STRESS INDEX (ESI) FOR DIFFERENT CLIMATIC CONDITIONS AND DISTANCES BELOW AND ABOVE SEA LEVEL				5. FUNDING NUMBERS
6. AUTHOR(S) Daniel S. Moran, Ph.D., Kent B. Pandolf, Ph.D., and Richard R. Gonzalez, Ph.D.				
7. PERFORMING ORGANIZATION NAME(S) AND ADDRESS(ES) U.S. Army Research Institute of Environmental Medicine Kansas St, BLDG 42 Natick, MA 01760-5007				8. PERFORMING ORGANIZATION REPORT NUMBER
9. SPONSORING / MONITORING AGENCY NAME(S) AND ADDRESS(ES) U.S. Army Medical Research and Materiel Command Fort Detrick, MD 21702				10. SPONSORING / MONITORING AGENCY REPORT NUMBER
11. SUPPLEMENTARY NOTES				
12a. DISTRIBUTION / AVAILABILITY STATEMENT Approved for Public Release; Distribution Unlimited				12b. DISTRIBUTION CODE
13. ABSTRACT (Maximum 200 words) This report summarizes the evaluation and refinement of an environmental stress index (ESI) for heat stress assessment. Two independent studies containing two different databases were analyzed in order to evaluate ESI for different climatic conditions and terrestrial distances below and above sea level. Meteorological measurements were analyzed in Study I at different climatic zones (hot/wet, hot/dry, and extremely hot/dry) at 19 different locations for 120 days; a modified ESI was developed as follows: $ESI = 0.62Ta - 0.007RH + 0.002SR + 0.0043(TaRH) - 0.078(0.1 + SR) - 1$ Where Ta = ambient temperature (°C), RH = relative humidity (%), and SR = solar radiation (Wm ⁻²). The correlation coefficients between ESI and the commonly used wet bulb globe temperature (WBGT) stress index were very high ($R^2 > 0.898$). ESI has the potential to be a practical alternative to the WBGT using fast response and accurate climatic microsensors (Ta, RH, SR) that can be combined in a portable device. Study II evaluated a new and small (5mm) light sensor (L) at different distances below and above sea level in order to measure global radiation (GR) applied in the ESI useful for heat stress assessment. Data were collected over 9 days during June-July from 6 different locations, from 09:00 through 17:00, from 3 instruments: L, pyranometer (P), and black globe. In general, analysis of the data revealed no significant differences between radiation measurements by P and L and between ESI calculated from L or P. We conclude that the L sensor has the potential to measure GR for use in heat stress assessment and in ESI at different distances below and above sea level.				
14. SUBJECT TERMS global thermal radiation; WBGT; prediction modeling; environmental stress index; low altitude thermal terrain evaluation				15. NUMBER OF PAGES 47
				16. PRICE CODE
17. SECURITY CLASSIFICATION OF REPORT Unclassified	18. SECURITY CLASSIFICATION OF THIS PAGE Unclassified	19. SECURITY CLASSIFICATION OF ABSTRACT Unclassified	20. LIMITATION OF ABSTRACT U	

TABLE OF CONTENTS

<u>SECTION</u>	<u>PAGE</u>
List of Figures.....	iv
List of Tables.....	vii
Acknowledgments.....	viii
List of Abbreviations.....	ix
Executive Summary.....	1
Introduction.....	2
Military Relevance.....	4
Methods.....	4
Study I.....	4
Study II.....	5
Results.....	6
Study I.....	6
Study II.....	27
Discussion.....	38
Study I.....	38
Study II.....	38
Conclusions.....	40
References.....	41
Appendix A.....	44
Appendix B.....	46
Appendix C.....	47

LIST OF FIGURES

<u>FIGURE</u>	<u>PAGE</u>
1	Comparison of the modified ESI with the WBGT index showing correlation (bottom) and residuals scattergram (top). Database for this figure was collected from station 1.....8
2	Comparison of the modified ESI with the WBGT index showing correlation (bottom) and residuals scattergram (top). Database for this figure was collected from station 2.....9
3	Comparison of the modified ESI with the WBGT index showing correlation (bottom) and residuals scattergram (top). Database for this figure was collected from station 3.....10
4	Comparison of the modified ESI with the WBGT index showing correlation (bottom) and residuals scattergram (top). Database for this figure was collected from station 4.....11
5	Comparison of the modified ESI with the WBGT index showing correlation (bottom) and residuals scattergram (top). Database for this figure was collected from station 5.....12
6	Comparison of the modified ESI with the WBGT index showing correlation (bottom) and residuals scattergram (top). Database for this figure was collected from station 6.....13
7	Comparison of the modified ESI with the WBGT index showing correlation (bottom) and residuals scattergram (top). Database for this figure was collected from station 7.....14
8	Comparison of the modified ESI with the WBGT index showing correlation (bottom) and residuals scattergram (top). Database for this figure was collected from station 815
9	Comparison of the modified ESI with the WBGT index showing correlation (bottom) and residuals scattergram (top). Database for this figure was collected from station 9.....16
10	Comparison of the modified ESI with the WBGT index showing correlation (bottom) and residuals scattergram (top). Database for this figure was collected from station 10.....17

<u>FIGURE</u>		<u>PAGE</u>
11	Comparison of the modified ESI with the WBGT index showing correlation (bottom) and residuals scattergram (top). Database for this figure was collected from station 11.....	18
12	Comparison of the modified ESI with the WBGT index showing correlation (bottom) and residuals scattergram (top). Database for this figure was collected from station 12.....	19
13	Comparison of the modified ESI with the WBGT index showing correlation (bottom) and residuals scattergram (top). Database for this figure was collected from station 13.....	20
14	Comparison of the modified ESI with the WBGT index showing correlation (bottom) and residuals scattergram (top). Database for this figure was collected from station 14.....	21
15	Comparison of the modified ESI with the WBGT index showing correlation (bottom) and residuals scattergram (top). Database for this figure was collected from station 15.....	22
16	Comparison of the modified ESI with the WBGT index showing correlation (bottom) and residuals scattergram (top). Database for this figure was collected from station 16.....	23
17	Comparison of the modified ESI with the WBGT index showing correlation (bottom) and residuals scattergram (top). Database for this figure was collected from station 17.....	24
18	Comparison of the modified ESI with the WBGT index showing correlation (bottom) and residuals scattergram (top). Database for this figure was collected from station 18.....	25
19	Comparison of the modified ESI with the WBGT index showing correlation (bottom) and residuals scattergram (top). Database for this figure was collected from station 19.....	26
20	Global radiation (GR) measured by 2 pyranometers (P, P _{IMS}), black globe thermometer (T _g), and 3 infra-red (IR) light sensors at -400m below sea level	28
21	Global radiation (GR) measured by pyranometer (P), T _g , and 3 IR light sensors at -200 m below sea level.....	29

FIGUREPAGE

22	Global radiation (GR) measured by 2 pyranometers (P, P _{IMS}), T _g , and 3 IR light sensors at 30m above sea level.....	30
23	Global radiation (GR) measured by pyranometer (P _{IMS}), T _g , and IR light sensor at 400m above sea level.....	31
24	Global radiation (GR) measured by 2 pyranometers (P, P _{IMS}), T _g , and 2 IR light sensors at 900m above sea level.....	32
25	Global radiation (GR) measured by pyranometer (P), T _g , and 2 IR light sensors at 1600m above sea level.....	33
26	Comparison of the modified ESI with the WBGT index. ESI was calculated from global radiation (GR) measured by pyranometer (ESI _P) and 3 different IR light sensors (ESI _{IR}) at -400 m below sea level.....	35
27	Comparison of the modified ESI with the WBGT index. ESI was calculated from GR measured by pyranometer (ESI _P) and 3 different IR light sensors (ESI _{IR}) at -200 m below sea level	35
28	Comparison of the modified ESI with the WBGT index. ESI was calculated from GR measured by pyranometer (ESI _P) and 3 different IR light sensors (ESI _{IR}) at 30m from sea level.....	36
29	Comparison of the modified ESI with the WBGT index. ESI was calculated from GR measured by pyranometer (ESI _P) and IR light sensor (ESI _{IR}) at 400m above sea level.....	36
30	Comparison of the modified ESI with the WBGT index. ESI was calculated from GR measured by pyranometer (ESI _P) and 2 different IR light sensors (ESI _{IR}) at 900m above sea level.....	37
31	Comparison of the modified ESI with the WBGT index. ESI was calculated from GR measured by pyranometer (ESI _P) and 2 different IR light sensors (ESI _{IR}) at 1600m above sea level.....	37

LIST OF TABLES

<u>TABLE</u>	<u>PAGE</u>
1	Mean (\pm SD) and range of all the environmental measurements from the 19 locations used for the ESI validation vs. the WBGT6
2	Mean (\pm SD) and range of global radiation (GR) measured using 2 pyranometers [by Heller Institute (P) and by Israeli Meteorological Service (P_{IMS})], black globe thermometer (T_g), and 3 infra-red (IR) light sensors. Database was collected from 6 different meteorological stations at different heights from sea level ($n=238$).....27
3	Mean (\pm SD) and range of the modified ESI and the WBGT index calculated from global radiation measured by pyranometer (ESI_P) and 3 different infra-red light sensors (ESI_{IR}).....34

ACKNOWLEDGMENTS

This work was conducted in Israel as part of a cooperative USARIEM - Israel Defence Force biophysics and biomedical modeling effort with the assistance of Mr. Ziv Hersch and Mr. Liran Mendel. Dr. Arie Laor and Ms. Liron Shalit's contributions in the statistical analysis and evaluation of the environmental stress index are appreciated. The authors are also extremely thankful for the cooperation and assistance of Mr. Jacob Mishaeli of the Israeli Meteorological Service.

LIST OF ABBREVIATIONS

DI – discomfort index

ESI – environmental stress index

GR – global radiation

IMS – Israeli Meteorological Service

IR – infra-red

MDI – modified discomfort index

RH – relative humidity

SL – solar load

SR – solar radiation

T_a – dry bulb temperature

T_g – black globe temperature

T_w – wet bulb temperature

WBGT – wet bulb globe temperature index

P – pyranometer

L – light sensor

EXECUTIVE SUMMARY

This report summarizes the evaluation and refinement of an environmental stress index (ESI) for heat stress assessment. Two independent studies containing two different databases were analyzed in order to evaluate ESI for different climatic conditions and terrestrial heights below and above sea level.

The purpose of the first study was to evaluate the ESI analytically and experimentally. Meteorological measurements were taken in different climatic zones (hot/wet, hot/dry, and extremely hot/dry) at 19 different locations for 120 days, and a modified ESI was developed as follows:

$$ESI=0.62T_a-0.007RH+0.002SR+0.0043(T_a\cdot RH)-0.078(0.1+SR)^{-1}$$

Where T_a = ambient temperature ($^{\circ}\text{C}$), RH = relative humidity (%), and SR = solar radiation ($\text{W}\cdot\text{m}^{-2}$). The correlation coefficients between ESI and the commonly used wet bulb globe temperature (WBGT) stress index were very high ($R^2>0.898$). Therefore, we concluded that ESI has the potential to be a practical alternative to the WBGT based on fast response and accurate climatic microsensors (T_a , RH , SR) that can be combined in a portable device.

The purpose of the second study was to evaluate the new and relatively small (5mm) light sensor (L) at different heights below and above sea level in order to measure global radiation (GR) applied in the ESI and for heat stress assessment. Data were collected over 9 days during June-July from 6 different locations, from 09:00 through 17:00, from 3 instruments: L, pyranometer (P), and black globe. In general, analysis of the data revealed no significant differences ($P>0.05$) between radiation measurements by P and L and between ESI calculated from L or P. Therefore, we concluded that the L sensor has the potential to measure GR for use in heat stress assessment and in ESI at different distances below and above sea level.

INTRODUCTION

Heat stress evaluation is generally determined through meteorological parameters that enable one to estimate the influence of several environmental factors on thermal comfort and physiological ability. The variables included in heat stress indices and their relative weights have changed over the years. Haldane (1905) developed an index for heat load and claimed that changes in the wet bulb thermometer alone were enough to integrate global heat load. Other environmental indices have also been suggested which include measurement of airflow and thermal radiation. Hill et al. (10) introduced the "Kata" thermometer, which enabled measurement of heat dissipation as a function of wind speed and other parameters. In 1932, Vernon (25) was the first to integrate radiant heat into an environmental stress index by using the globe thermometer.

Yaglou and Minard (27) first introduced the wet bulb globe temperature (WBGT) during an extensive period of development of heat stress indices in the first half of the 20th century. The WBGT index gained popularity mainly due to its simplicity and convenience of use and soon was considered the most common heat stress index for describing environmental heat stress. This index is obtained from three parameters: black globe temperature (T_g), which considers the solar radiation; wet bulb temperature (T_w); and dry bulb temperature (T_a), and is calculated as follows: $WBGT = 0.7T_w + 0.2T_g + 0.1T_a$. WBGT has gained immense popularity over the years and has been in use in the field by the U.S. Army. It is the index on which sports associations base training safety orders as guidance to prevent heat injury (1, 3, 13, 14, 15). The World Health Organization (WHO) has also adopted it. In 1972, the National Institute for Occupational Safety and Health (NIOSH) established the WBGT as the criterion for determining occupational exposure to a hot environment (18). In 1982, WBGT was approved by the ISO as an international standard for heat load assessment, and it is commonly used as a safety index for workers in various occupations (4, 5, 8, 20). Later, work-rest regime regulations were made based on this index. However, WBGT is limited in its evaluation of heat stress due to the inconvenience of measuring T_g . The T_g is usually measured by a thermometer surrounded by a 6" blackened sphere, and purportedly integrates the global radiation component of the thermal load. However, measuring T_g is cumbersome in many circumstances for two main reasons. First, T_g measurement requires about 30 min for the instrument to reach equilibrium. Second, the blackened sphere is often too large for specialized spaces like helicopter cockpits or armored vehicles. Therefore, measuring T_g becomes impractical, especially in transient situations.

At the time WBGT was introduced, many empirical indices were developed that originated from the old effective temperature (ET), the corrected ET (CET), the modified ET (MET), and the equivalent ET (ETR) (2, 11, 26). All of these indices were based on T_a , T_w , and T_g , but none was ever associated with any physiological variable. The WBGT has been only partly evaluated by analyzing the association between heat stroke cases in soldiers and the heat load assessed by the WBGT (27). In fact, there is no known laboratory- controlled study where the WBGT was evaluated. Recently, Moran et al.

(16) introduced a new environmental stress index (ESI) based on measurements of T_a , relative humidity (RH), and solar radiation (SR). ESI was highly correlated with the WBGT index (16). The ESI as a stress index, for the first time, incorporates direct measurements of SR and RH. Additionally, all the three meteorological variables that make up the ESI are characterized by fast reading sensors easily obtained commercially. However, ESI needs to be further evaluated and validated under different climatic and topographical conditions.

The flow of global radiation falling to the earth's surface is dependent on four factors. The first factor is astronomical, influenced by the distance of the sun from the measured site and the length of daylight. The distance of the sun from a site is dependent on the topographical height of the surface and the hour of the day. With higher topographical height, thermal radiation becomes more intense. Thermal radiation is also more intense as daylight becomes extended. The second factor is the transparency of the atmosphere. This is a measurement, which changes daily and monthly. Radiation is more intense as atmosphere becomes clearer. The third important factor is the amount of clouds in the sky. Cloudy skies greatly influence the measured global radiation. With cloudy skies, thermal radiation becomes weaker. Cloudiness, of course, changes as the seasons change during the year, but it can also change daily. The fourth and final factor is the surface coverage (Albedo). Different types of surfaces are influenced in variable ways depending on the reflected solar radiation. The more light is reflected from an exterior surface, the greater the measured radiation. A snow-covered surface is a good example of a surface greatly influenced by the reflected radiation. Here the measured radiation is greater than a blackened surface that absorbs the sun's radiation. Therefore, any device required to measure solar radiation should also be validated by all these factors.

Over the last few years, major progress has been made in the field of portable heat load instrument technology. New instruments are able to measure and present a variety of meteorological parameters (e.g., T_a , RH, and wind speed) and display the calculated heat load on a screen. Moreover, no special training is needed to operate these instruments. It is worth mentioning that the microsensors in these instruments have a fast response time, and displaying the results is a matter of waiting just a few seconds. The simplicity of operation makes these instruments previously inaccessible to laymen.

There were two purposes for the present study. The first was to evaluate and validate, using a large database, the thermal load index (ESI) constructed from microsensors for T_a , RH and solar radiation (SR), and to assess and determine whether this newly developed index can serve as a reliable and valid alternative to WBGT for measuring environmental stress. The second purpose was to evaluate a new and relatively small (5 mm) light sensor (L) that is easily deployable at different heights above sea level in order to measure global radiation in the ESI.

MILITARY RELEVANCE

It is important for military commanders to have knowledge in real-time about environmental stress occurring during different scenarios (e.g., during training, combat and deployments to hot/cold environments). Current techniques of evaluating environmental stress are not facile. They are also cumbersome, labor intensive, time consuming, and do not use modern technology or advanced sensor systems for weather measurements. Current systems with reliable microsensors also have not been fully integrated with microprocessor units into a portable, ultra lightweight, friendly to use device.

The existing U.S. military heat stress monitoring systems are based largely on the WBGT (14), whereas the IDF system is based on the DI (22). The inherent limitations of the WBGT and the DI have been reported (7,12,15) in terms of applicability across a broad range of potential military scenarios and environments. These limitations are attributed, in part, to early constraints on sensor and computational complexity.

Mathematical models of human heat strain allow full consideration of the complex interactions of environment, clothing, acclimatization status, and metabolic heat production that ultimately determine a soldier's performance limits in a given scenario.

METHODS

STUDY I

The database was obtained from a study collected at various climatic sites in Israel and contained 126,558 measurements for each of the variables measured. Weather measurements were collected every 10 min, during 24 hours a day, for 120 days, at 19 different locations around Israel, including sites near the Mediterranean sea characterized as a high humidity zone, sites in the desert characterized as a hot/dry zone, and sites near the Red Sea characterized as an extremely hot/dry zone.

Measurements

The official Israeli Meteorological Service collected weather measurements for the nineteen locations. T_a and T_w were measured with Campbell thermometers (model HMP45C), and relative humidity (RH) was measured with a Rotronic instrument (model, MP 100A). These three instruments were placed under a shelter (Stevenson screen). Under open sky, T_g was measured using the Vernon black globe thermometer, solar radiation (SR) was measured using the EPLAB radiometer (sensitivity of 285-2800 nm), and the infra-red (IR) light sensor measured by Centro Vision sensor (model CD-1705) with peak sensitivity of 800-920 nm.

Calculations

Heat stress indices were calculated as follows: WBGT was calculated according to Yaglou and Minard's standard formula; $WBGT = 0.7T_w + 0.2T_g + 0.1T_a$ (22). The newly modified environmental stress index (ESI) was calculated as follows:

$$ESI = 0.62T_a - 0.007RH + 0.002SR + 0.0043(T_a \cdot RH) - 0.078(0.1 + SR)^{-1}$$

Statistical Analysis

For the evaluation of the modified ESI, we validated a series of models for WBGT as dependent variables, and T_a , RH, SR, their interactions and different transformations (inverse, and quadratic) as independent variables. Pearson's analysis was used for testing bivariate correlations between the independent and the dependent variables. All models were linear models and used the least squares algorithm. Optimization of the constants was executed by the DUD (does not use derivative) method (19). For all models, we computed the coefficient of determination (R-Square of the model) and plotted a series of residual plots versus predicted values for all data and for every meteorological station separately. All statistical contrasts were accepted at the $P < 0.05$ level of significance. Data are presented in this study as means \pm SE. For all computations and statistical analysis, we used SAS 8.0 Software, Procedures CORR and GLM.

STUDY II

This database was obtained from a study conducted in Israel, during the summer season (June-July) for 9 days at 6 different meteorological stations at different terrestrial heights, from the lowest place in the world at -400m, located at the Dead Sea, and up to 1600m, located at a ski resort in Mt. Hermon. Global or solar radiation measurements were collected for 15-min daily between 09:00 and 17:00. These data were collected from the following three instruments placed under the open sky at 1 m height: black globe (T_g) using the Vernon-black globe thermometer, EPLAB pyranometer (P), and infra-red light (IRL) sensor.

Statistical Analysis

The new model to predict P values from L data was validated as a linear model that was fitted by the least square method using SAS 8.0 software. Correlation coefficients between ESI calculated from P (ESI_P) and IRL sensor (ESI_{IR}) were computed using Pearson correlation analysis. All statistical contrasts were accepted at the $P < 0.01$ level of significance.

RESULTS

STUDY I

These data were collected every 15 min over 24 hr for 120 days. Therefore, a wide range of weather measurements, over 126,000 for each variable, was covered as depicted in Table 1 (mean \pm SD), and for each of the 19 stations in Appendix A.

Table 1. Mean (\pm SD) and range of environmental measurements of the ESI validation versus the WBGT. Data were collected from 19 different locations every 15 min over 24 hours for 120 days.

	T_a (°C)	T_w (°C)	RH (%)	T_g (°C)	SR (W·m ⁻²)	WBGT (°C)
Mean \pm SD	23.07 \pm 6.35	16.88 \pm 3.66	55.52 \pm 24.00	26.40 \pm 10.81	289 \pm 353	19.05 \pm 4.71
Range	0.80-44.30	0.60-29.70	1.75-100	0-59.42	0-1337	0.7-32.58

In order to better correlate ESI with WBGT and to improve the distribution around the line of identity, we modified the ESI constants. This newly modified ESI is based on the same three variables (T_a , RH, and SR), interaction ($T_a \cdot RH$) and transformation $[(SR+0.1)^{-1}]$ as the original ESI (16). The ESI modification is a result of statistical analysis, which included three steps. The first step applied the original ESI on the 19 different databases and analyzed them for correlation between WBGT and ESI, and the residual scattergram from the line of identity. In the second step, we validated the WBGT as a dependent variable, and each of the variables and components in the original ESI as an independent variable. Since the results from the second step revealed a very high correlation between the dependent and the independent variables, we progressed to the third step. At the second stage, the ESI concept and construction was evaluated. For the third step, we optimized the different constants of the ESI variables, interaction and transformation as follows:

For T_a measured in °C:

$$ESI=0.62T_a-0.007RH+0.002SR+0.0043(T_a \cdot RH)-0.078(0.1+SR)^{-1}$$

For T_a measured in °F:

$$ESI=0.73T_a-0.007RH+0.005SR+0.0026(T_a \cdot RH)-0.115(0.1+SR)^{-1}$$

The modified ESI was applied separately to each of the 19 databases, and overall, a highly significant correlation coefficient ($R^2 \geq 0.898$, $P < 0.001$) was obtained with residuals distributed symmetrically around the zero line in most of the locations as depicted in Figures 1-19.

Figure 1. Comparison of the modified ESI with the WBGT index showing correlation (bottom) and residuals scattergram (top). Database for this figure was collected from station 1

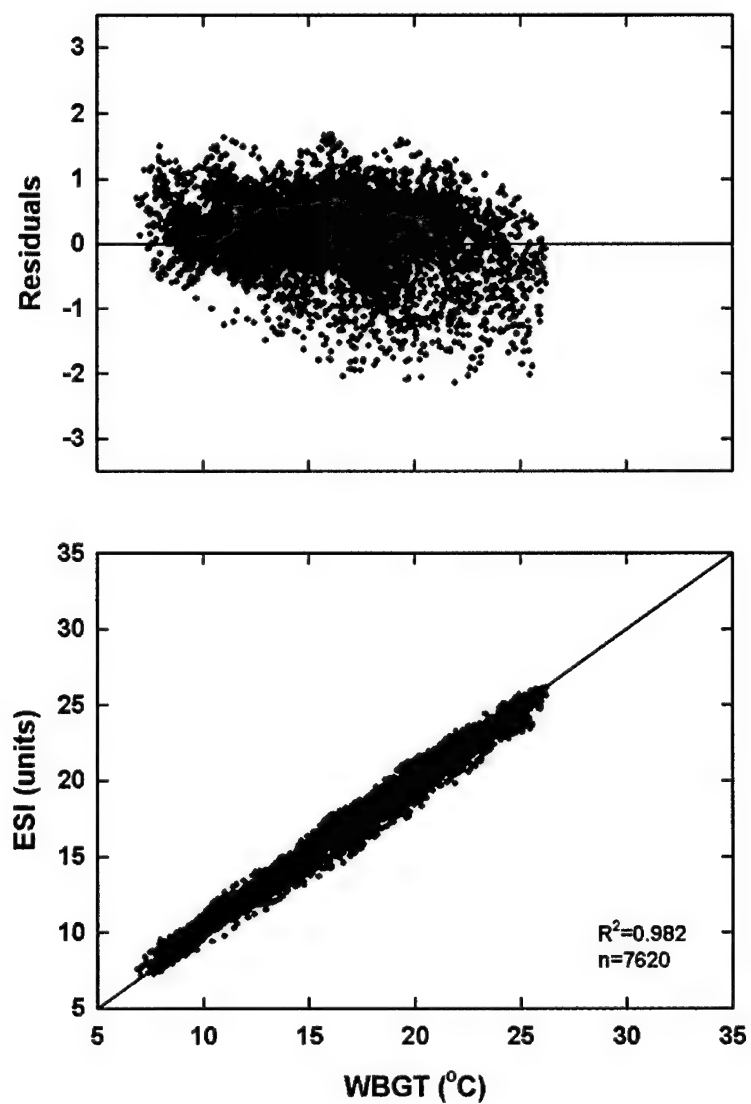


Figure 2. Comparison of the modified ESI with the WBGT index showing correlation (bottom) and residuals scattergram (top). Database for this figure was collected from station 2

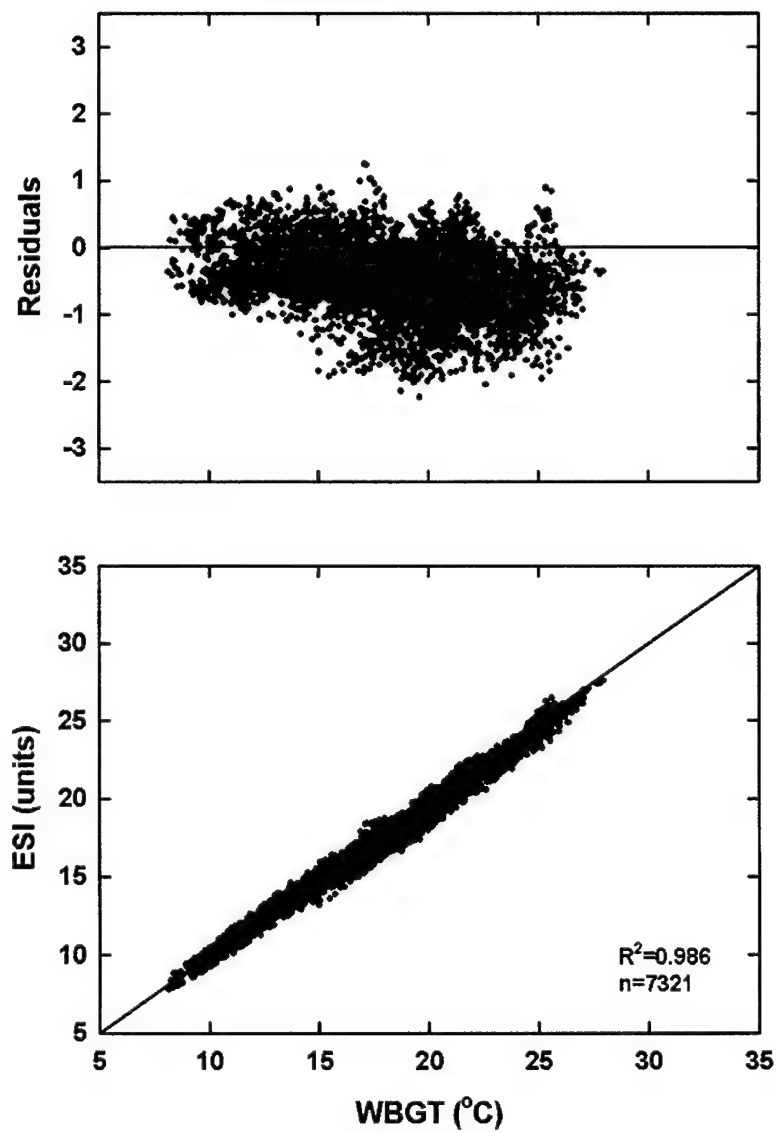


Figure 3. Comparison of the modified ESI with the WBGT index showing correlation (bottom) and residuals scattergram (top). Database for this figure was collected from station 3

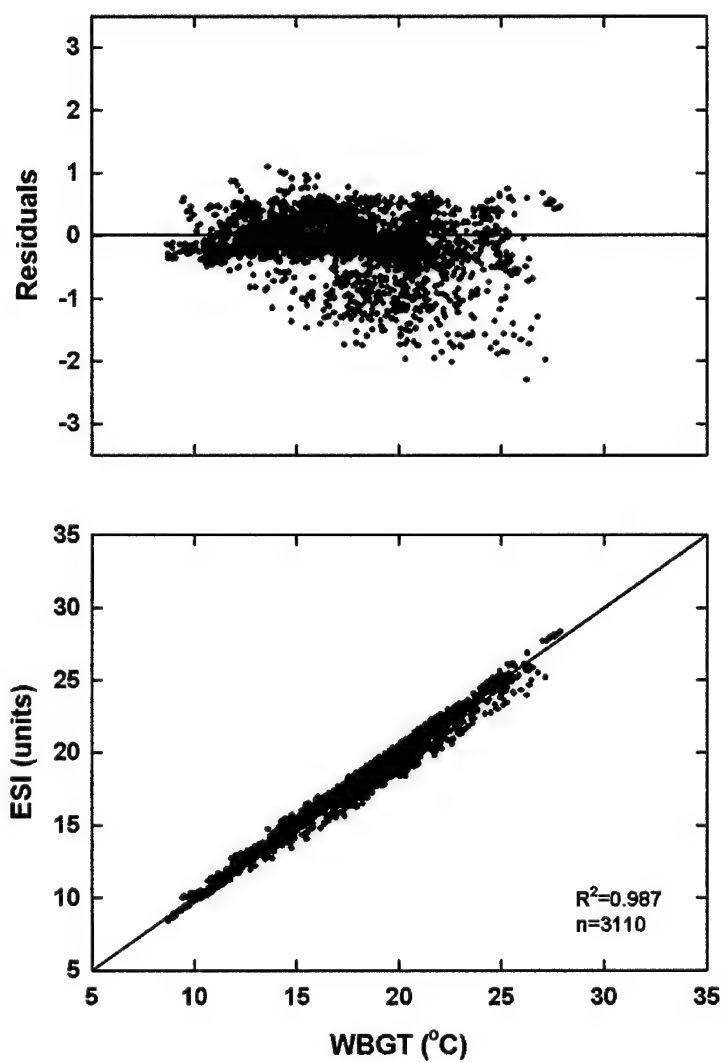


Figure 4. Comparison of the modified ESI with the WBGT index showing correlation (bottom) and residuals scattergram (top). Database for this figure was collected from station 4

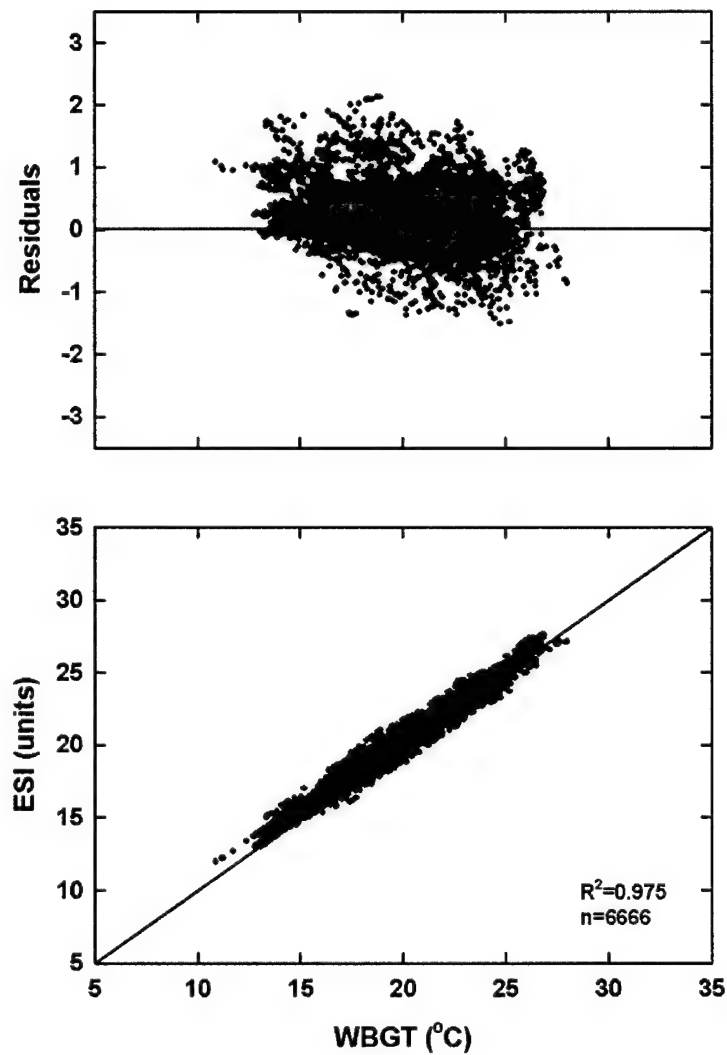


Figure 5. Comparison of the modified ESI with the WBGT index showing correlation (bottom) and residuals scattergram (top). Database for this figure was collected from station 5

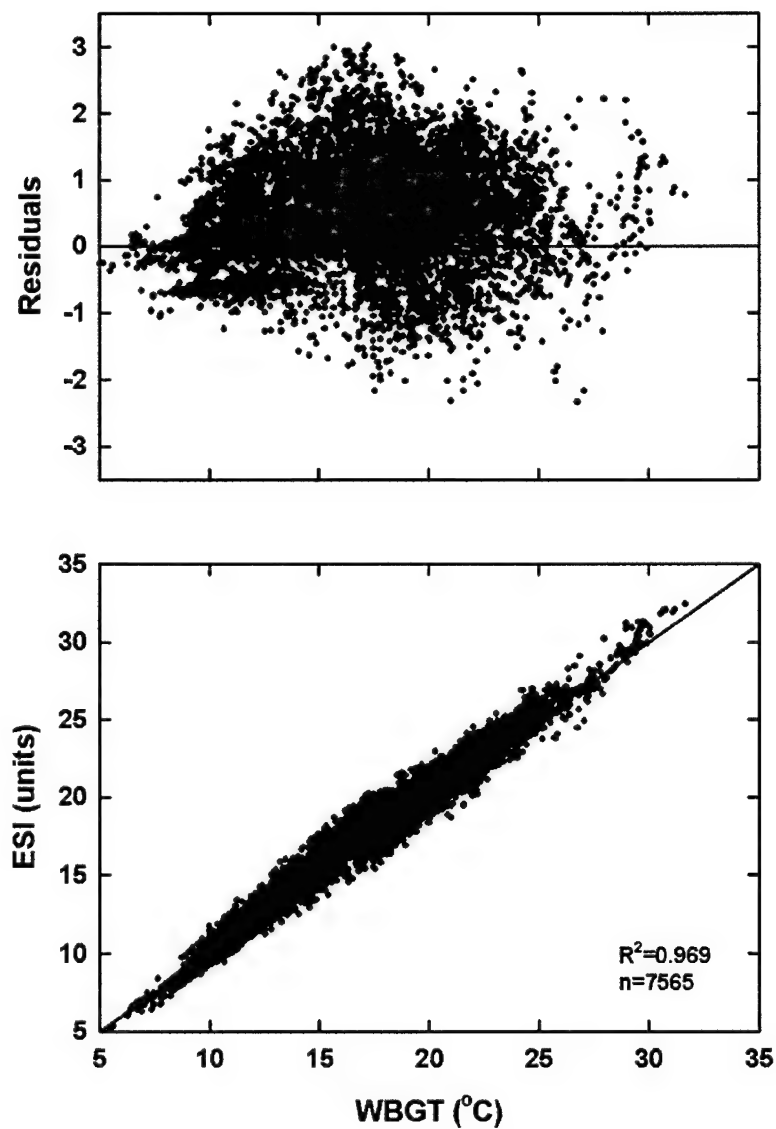


Figure 6. Comparison of the modified ESI with the WBGT index showing correlation (bottom) and residuals scattergram (top). Database for this figure was collected from station 6

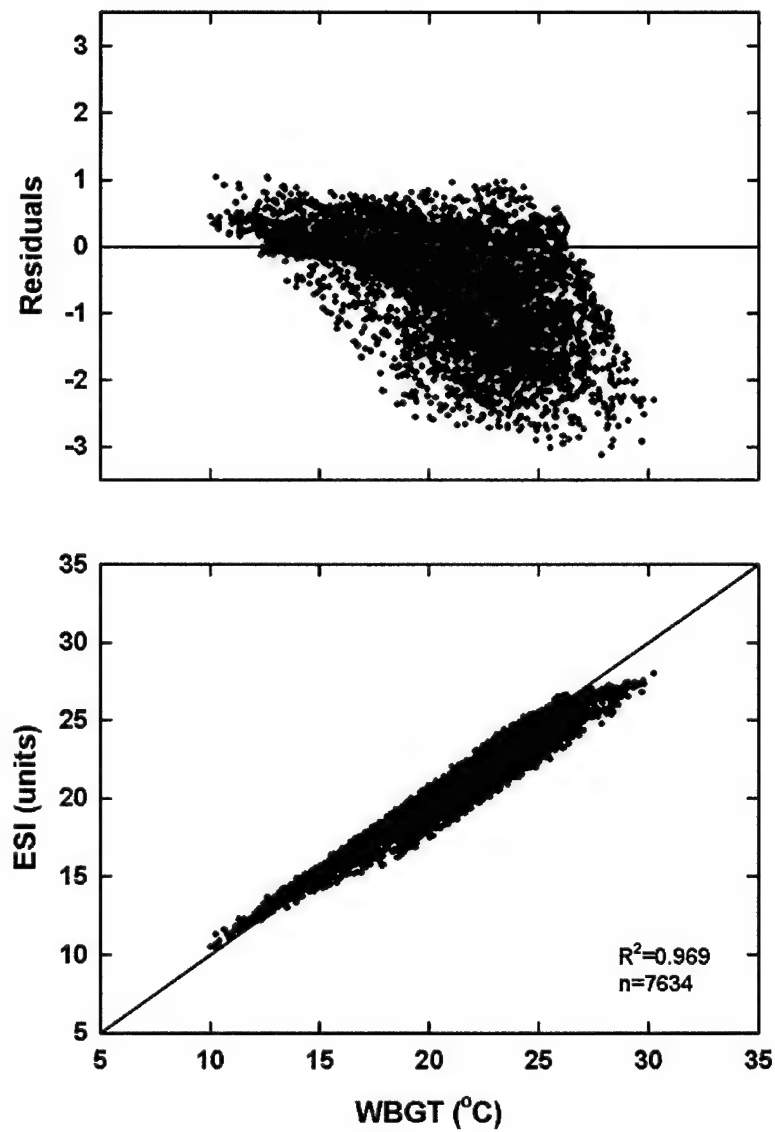


Figure 7. Comparison of the modified ESI with the WBGT index showing correlation (bottom) and residuals scattergram (top). Database for this figure was collected from station 7

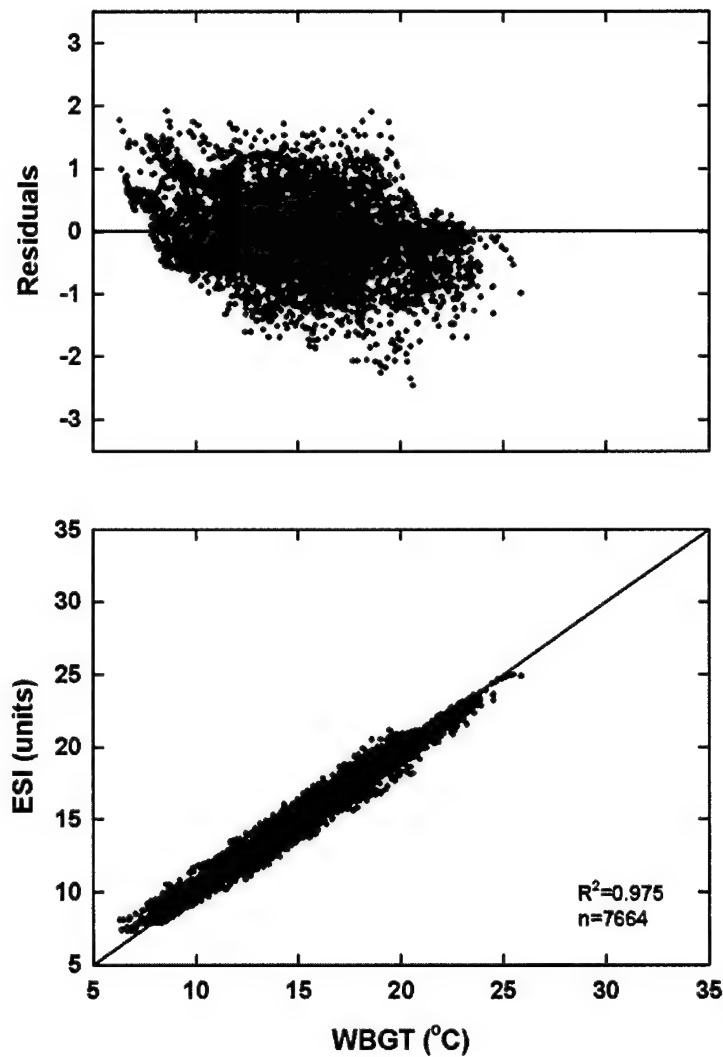


Figure 8. Comparison of the modified ESI with the WBGT index showing correlation (bottom) and residuals scattergram (top). Database for this figure was collected from station 8

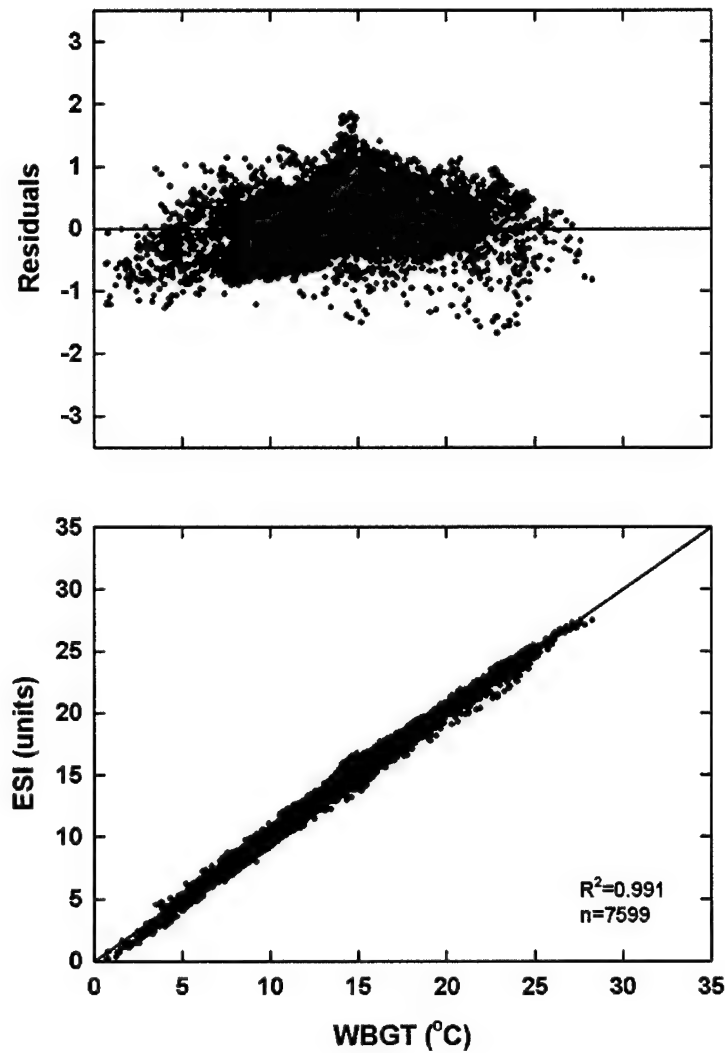


Figure 9. Comparison of the modified ESI with the WBGT index showing correlation (bottom) and residuals scattergram (top). Database for this figure was collected from station 9

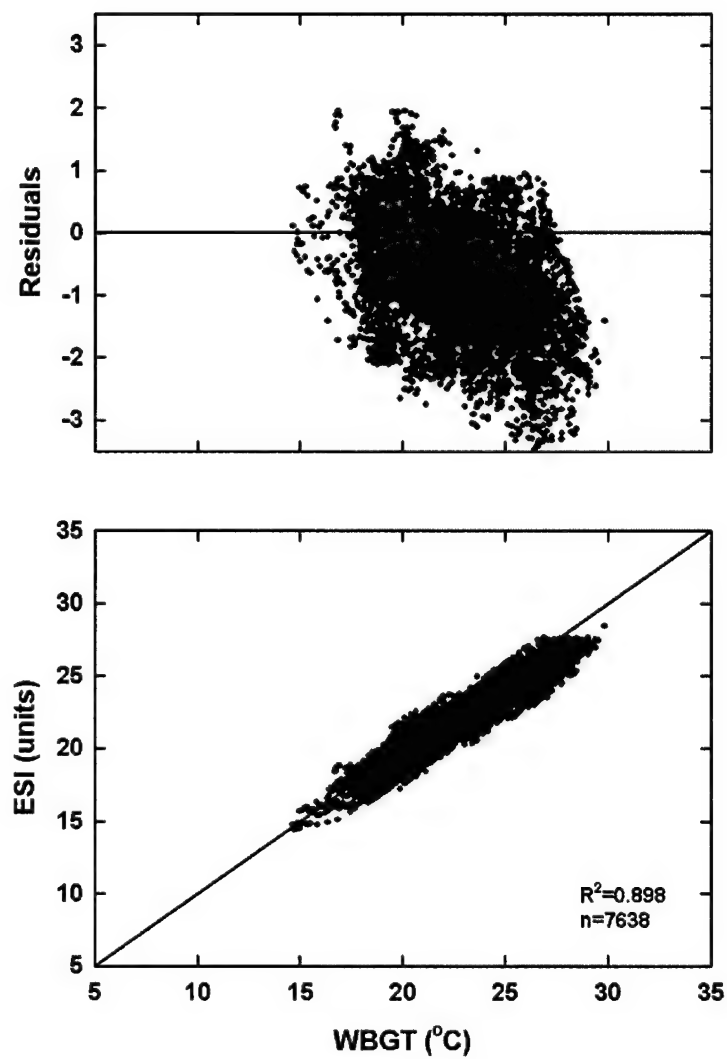


Figure 10. Comparison of the modified ESI with the WBGT index showing correlation (bottom) and residuals scattergram (top). Database for this figure was collected from station 10

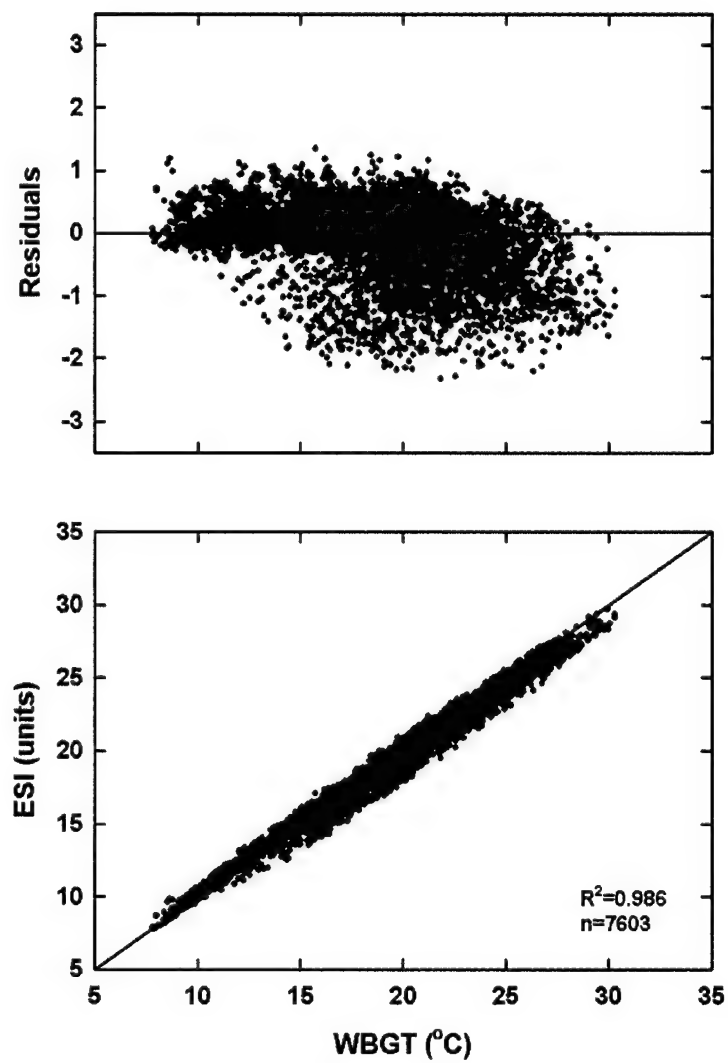


Figure 11. Comparison of the modified ESI with the WBGT index showing correlation (bottom) and residuals scattergram (top). Database for this figure was collected from station 11

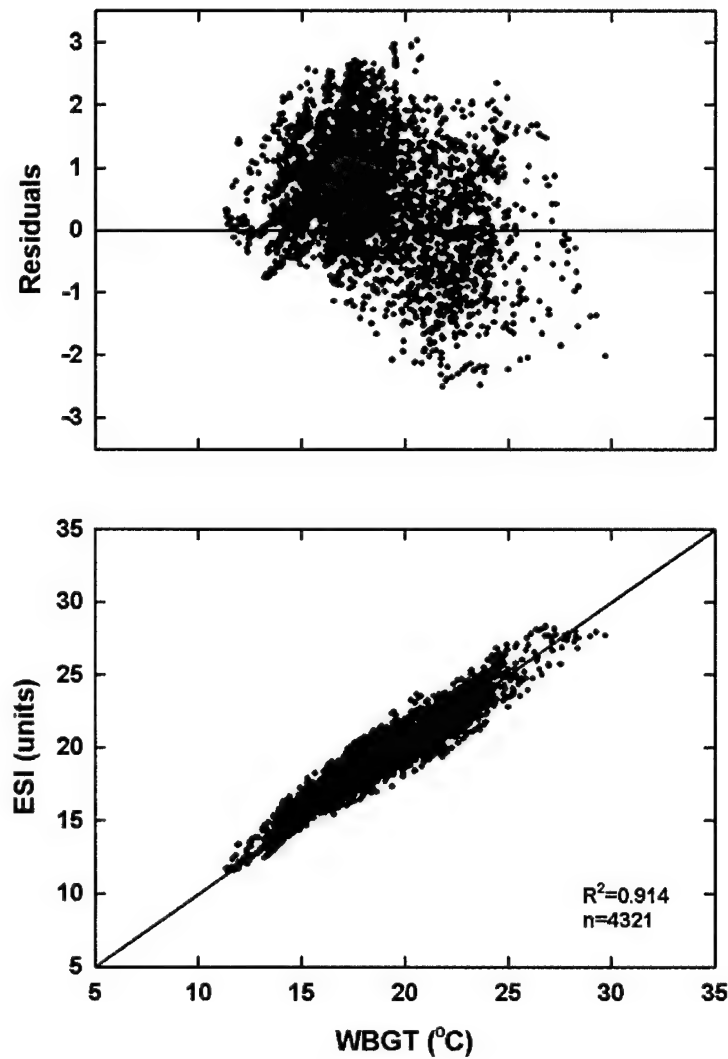


Figure 12. Comparison of the modified ESI with the WBGT index showing correlation (bottom) and residuals scattergram (top). Database for this figure was collected from station 12

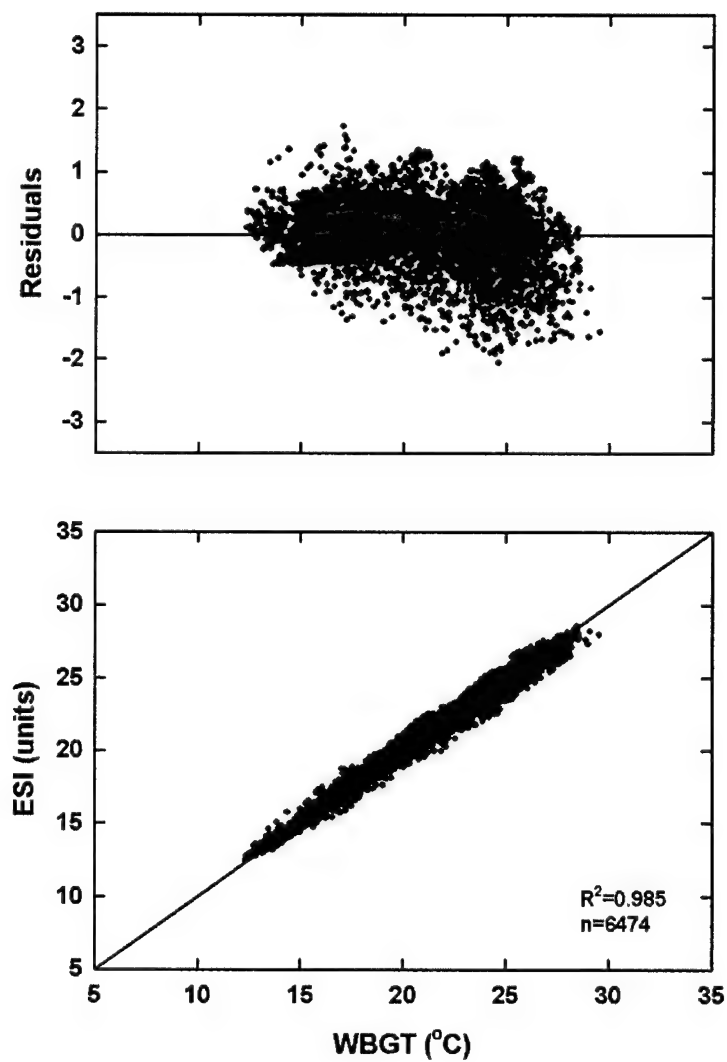


Figure 13. Comparison of the modified ESI with the WBGT index showing correlation (bottom) and residuals scattergram (top). Database for this figure was collected from station 13

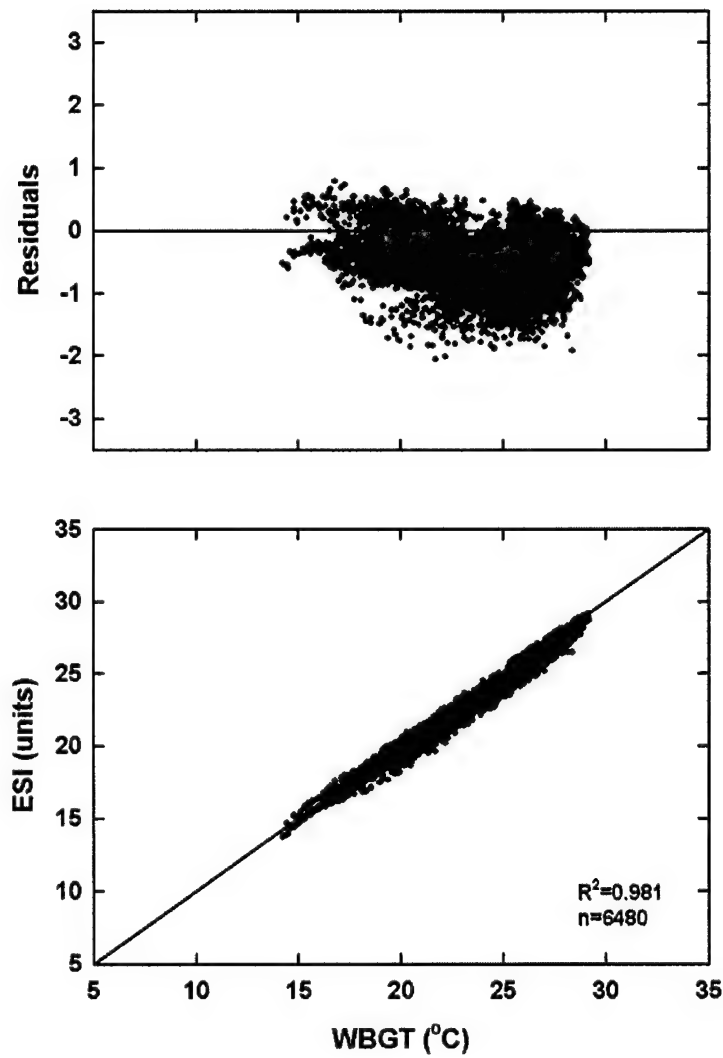


Figure 14. Comparison of the modified ESI with the WBGT index showing correlation (bottom) and residuals scattergram (top). Database for this figure was collected from station 14

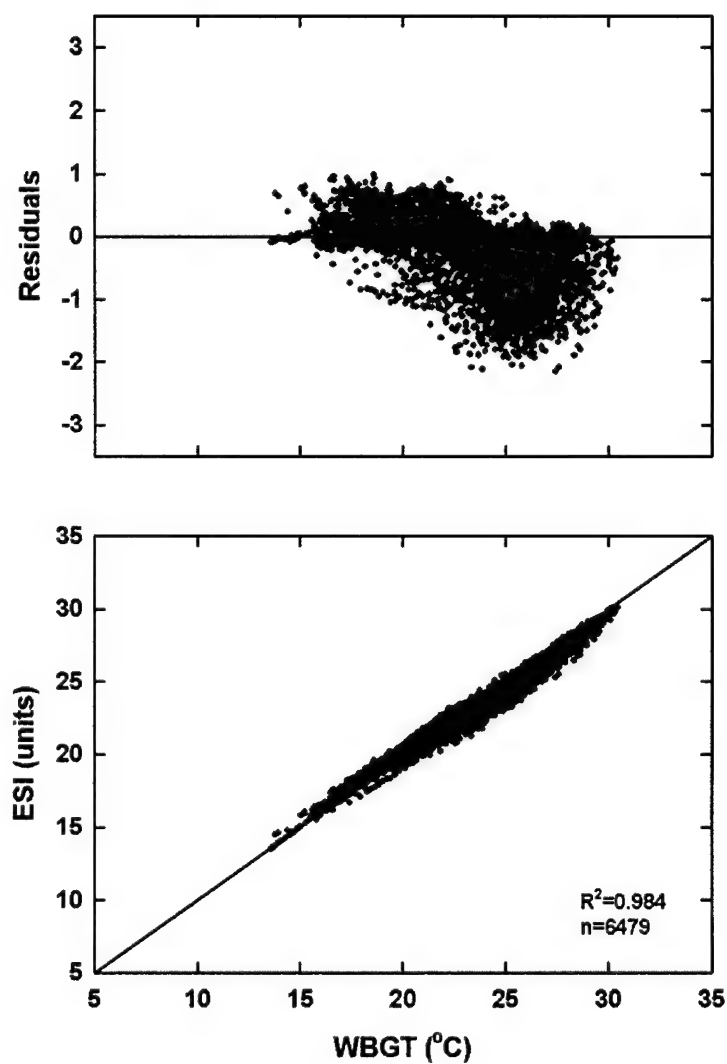


Figure 15. Comparison of the modified ESI with the WBGT index showing correlation (bottom) and residuals scattergram (top). Database for this figure was collected from station 15

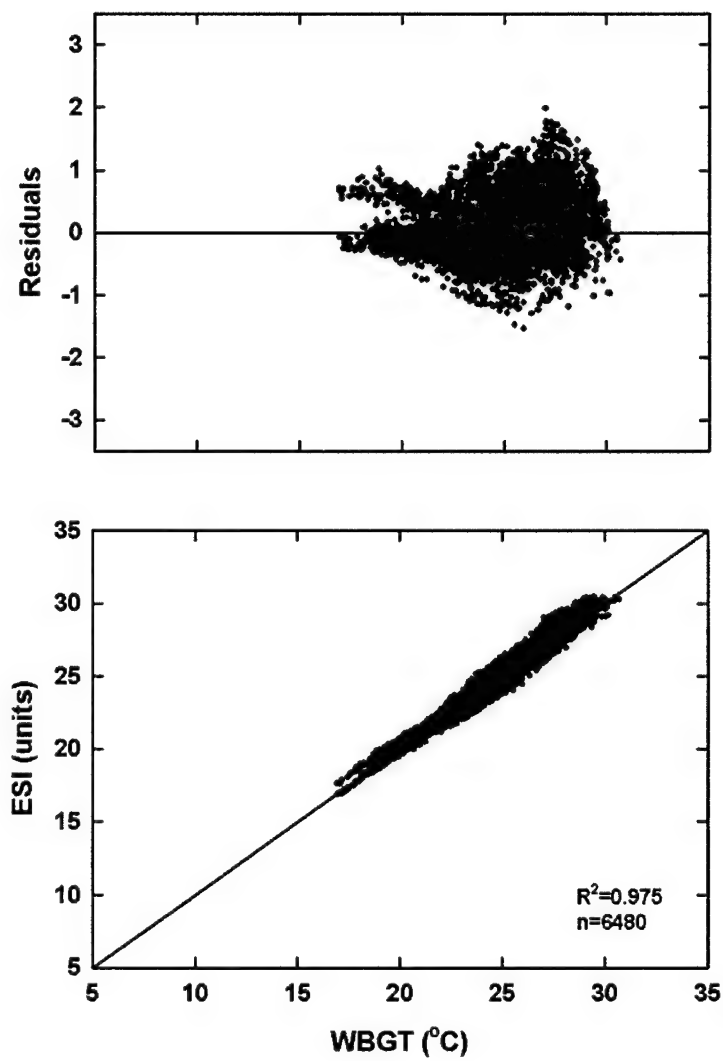


Figure 16. Comparison of the modified ESI with the WBGT index showing correlation (bottom) and residuals scattergram (top). Database for this figure was collected from station 16

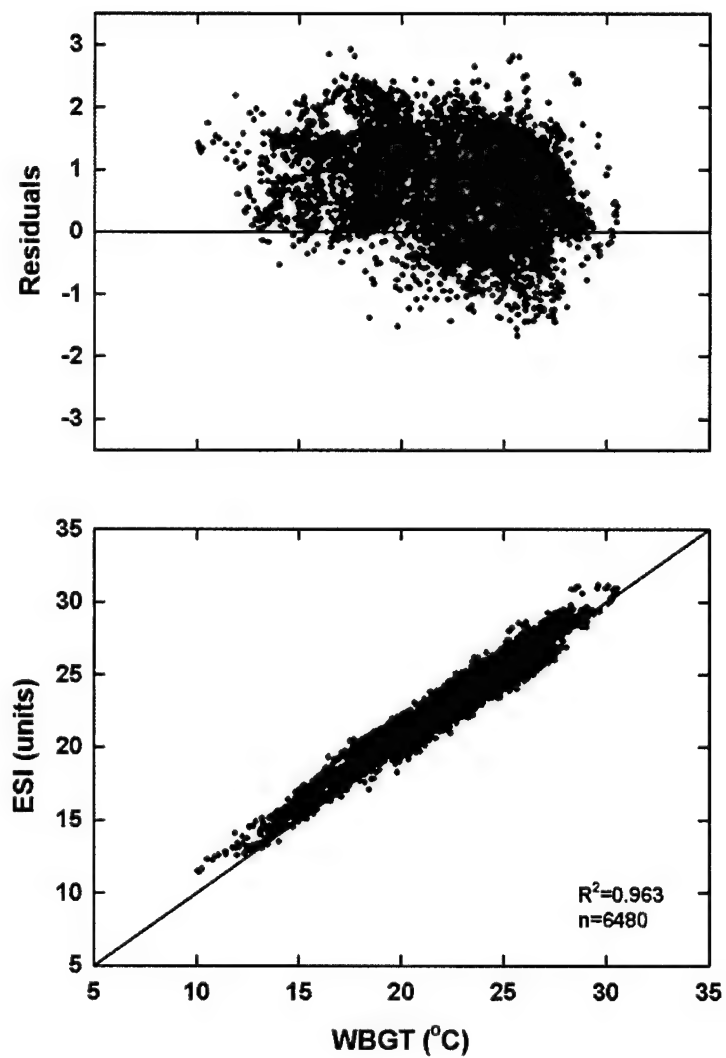


Figure 17. Comparison of the modified ESI with the WBGT index showing correlation (bottom) and residuals scattergram (top). Database for this figure was collected from station 17

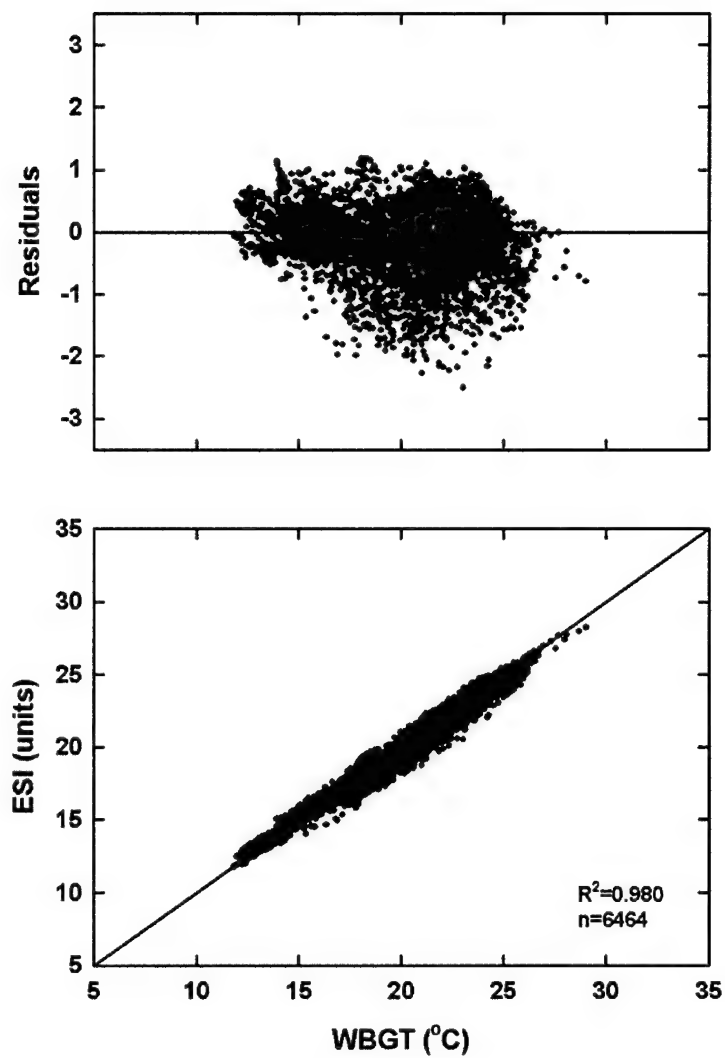


Figure 18. Comparison of the modified ESI with the WBGT index showing correlation (bottom) and residuals scattergram (top). Database for this figure was collected from station 18

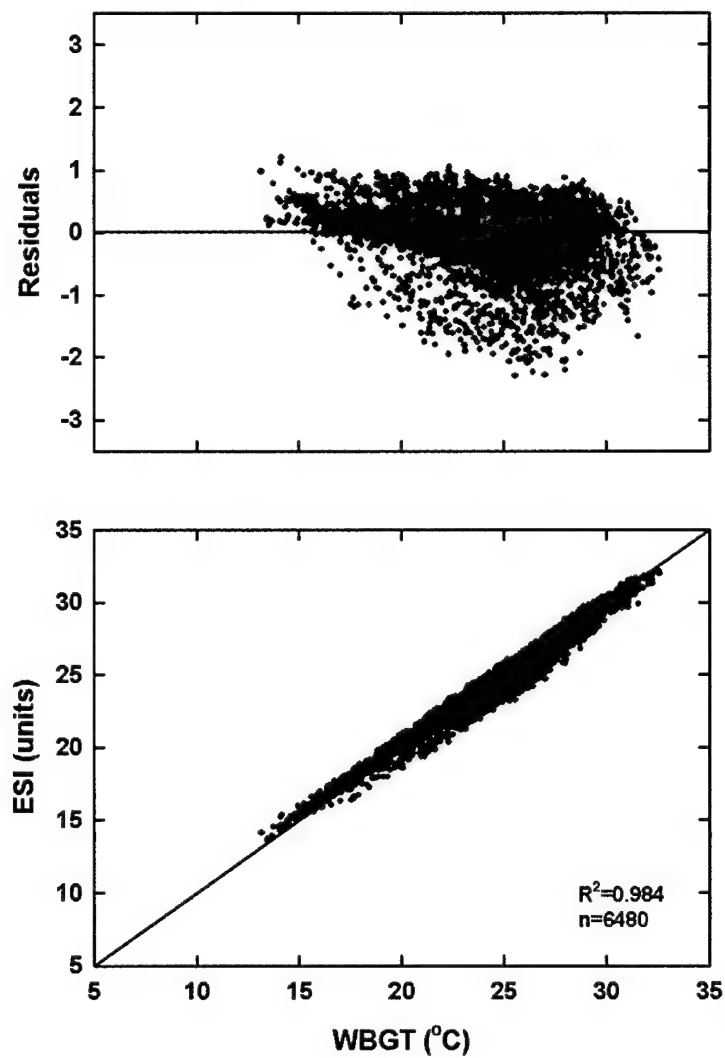
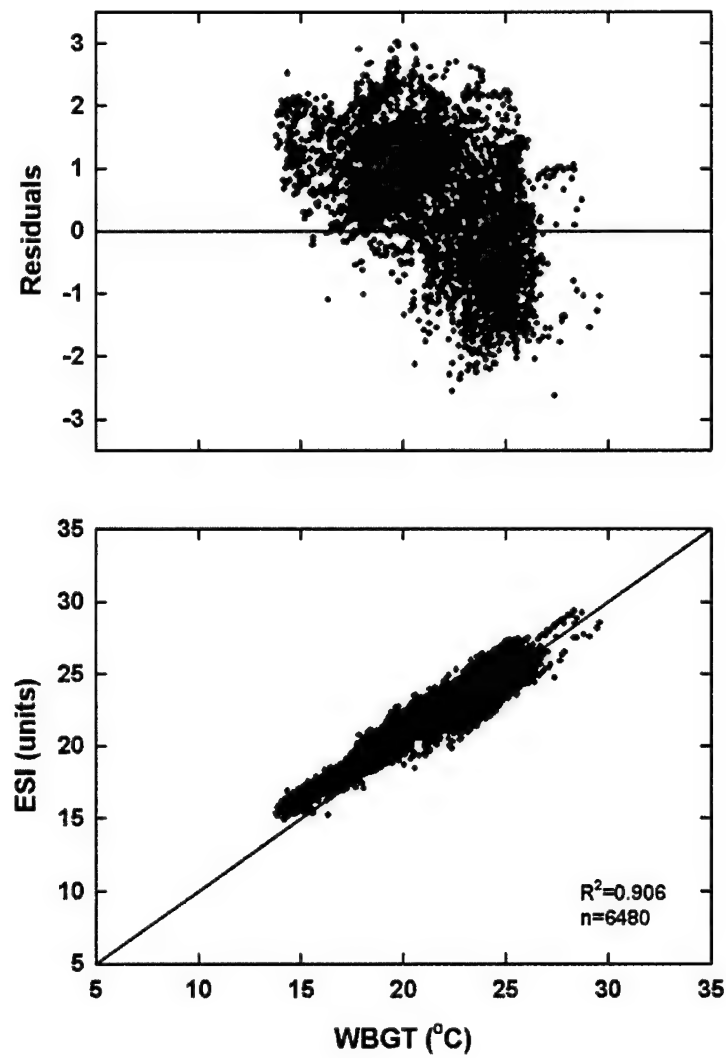


Figure 19. Comparison of the modified ESI with the WBGT index showing correlation (bottom) and residuals scattergram (top). Database for this figure was collected from station 19



STUDY II

The dataset collected in this study included global radiation measured by pyranometer (P), infra-red (IR) light sensor, and black globe thermometer (T_g), wet bulb temperature (T_w), and ambient temperature (T_a). The measurements were carried out over a wide range of weather measurements as depicted in Table 2 for mean \pm SD values and in Appendix B for each of the 6 locations.

There were no significant differences (NS, $P>0.05$) between the measurements of the three IR sensors as depicted in Table 2 and for each of the 6 locations in Appendix B. However, higher values for the pyranometer in comparison to the 3 IR sensors measurements were found mainly between 11:00 and 14:00 at the 6 different locations (see Figures 20-25). Analysis of the T_g measurements showed similar patterns as in the radiation sensors (P and L) measurements.

Table 2. Mean (\pm SD) and range of global radiation (GR) measured using 2 pyranometers [by Heller Institute] (P) and by Israeli Meteorological Service (P_{IMS})], black globe thermometer (T_g), and 3 infra-red (IR) light sensor. Database was collected from 6 different meteorological stations at various distances below (-200 m and -400 m) and above sea level ($n=238$).

	P	P_{IMS}	T_g	IR ₁	IR ₂	IR ₃	T_a	T_w
	(W·m ⁻²)	(W·m ⁻²)	(°C)	(W·m ⁻²)	(W·m ⁻²)	(W·m ⁻²)	(°C)	(°C)
Mean	754 \pm	818 \pm	42.35 \pm	651 \pm	639 \pm	665 \pm	28.69 \pm	21.52 \pm
\pm SD	189	254	4.76	172	158	157	4.39	2.14
Range	205-1028	40-1058	30-52	151-875	160-876	179-887	19.1-38.6	16.5-26.0

Figure 20. Global radiation (GR) measured by 2 pyranometers (P, P_{IMS}), black globe thermometer (T_g), and 3 infra-red (IR) light sensors at -400 m below sea level

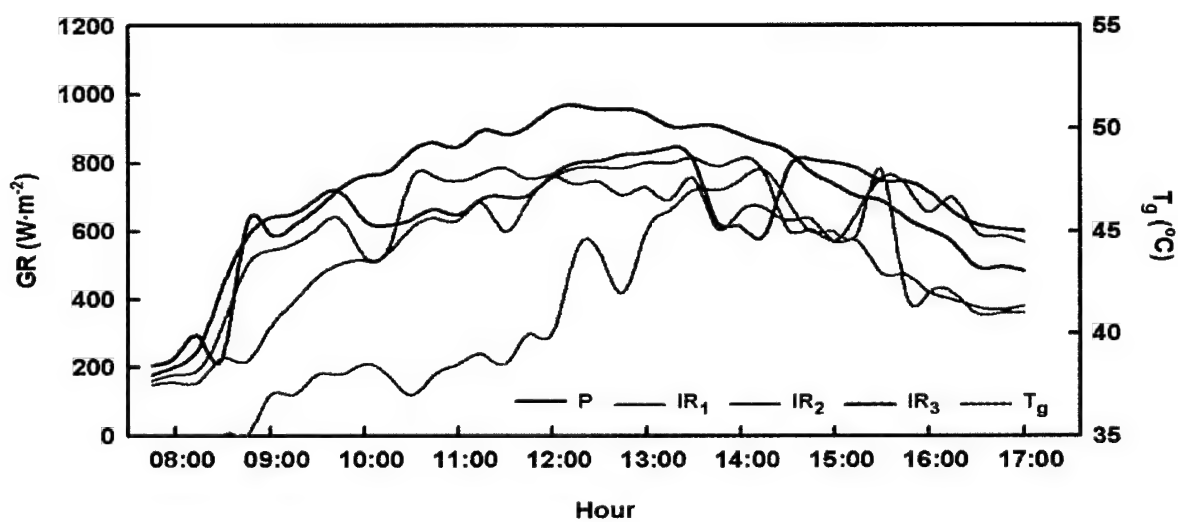


Figure 21: Global radiation (GR) measured by pyranometer (P), 3 infra-red (IR) light sensors and black globe thermometer (T_g) at -200 m below sea level.

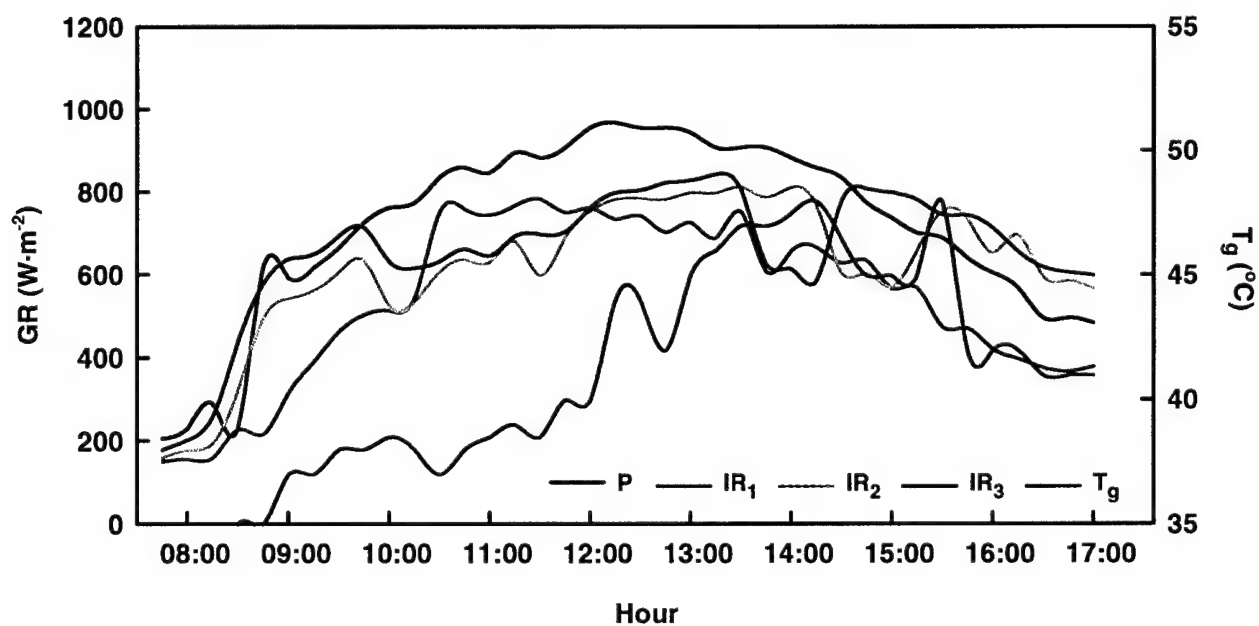


Figure 22: Global radiation (GR) measured by 2 pyranometers (P, P_{IMS}), 3 infra-red (IR) light sensors and black globe thermometer (T_g) at 30 m from sea level.

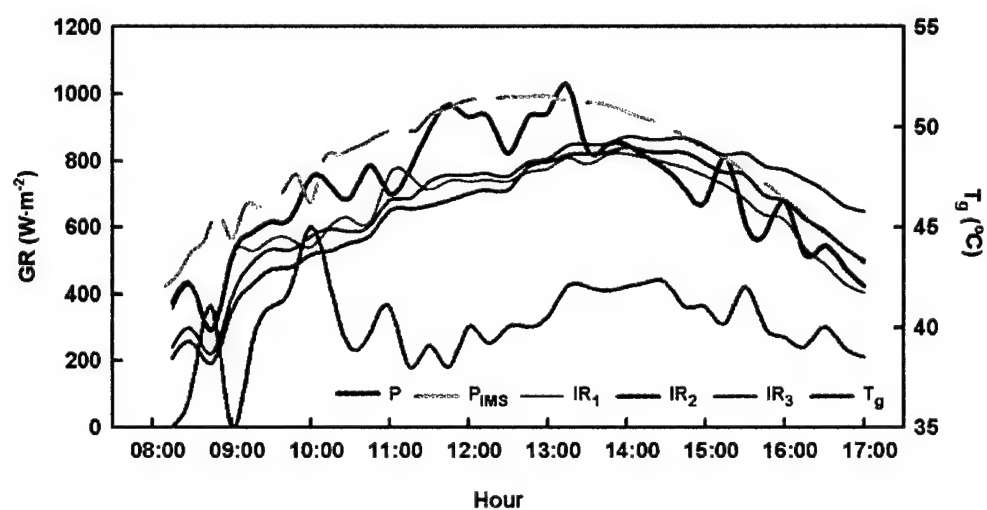


Figure 23: Global radiation (GR) measured by pyranometer (P_{IMS}), infra-red (IR) light sensor and black globe thermometer (T_g) at 400 m from sea level.

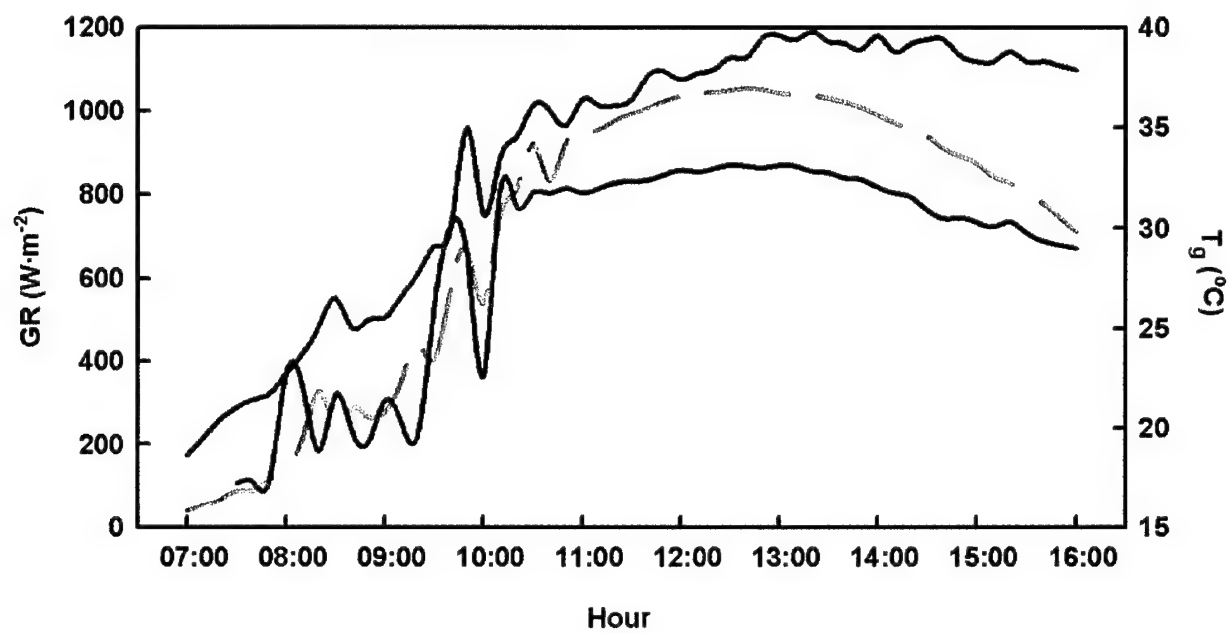
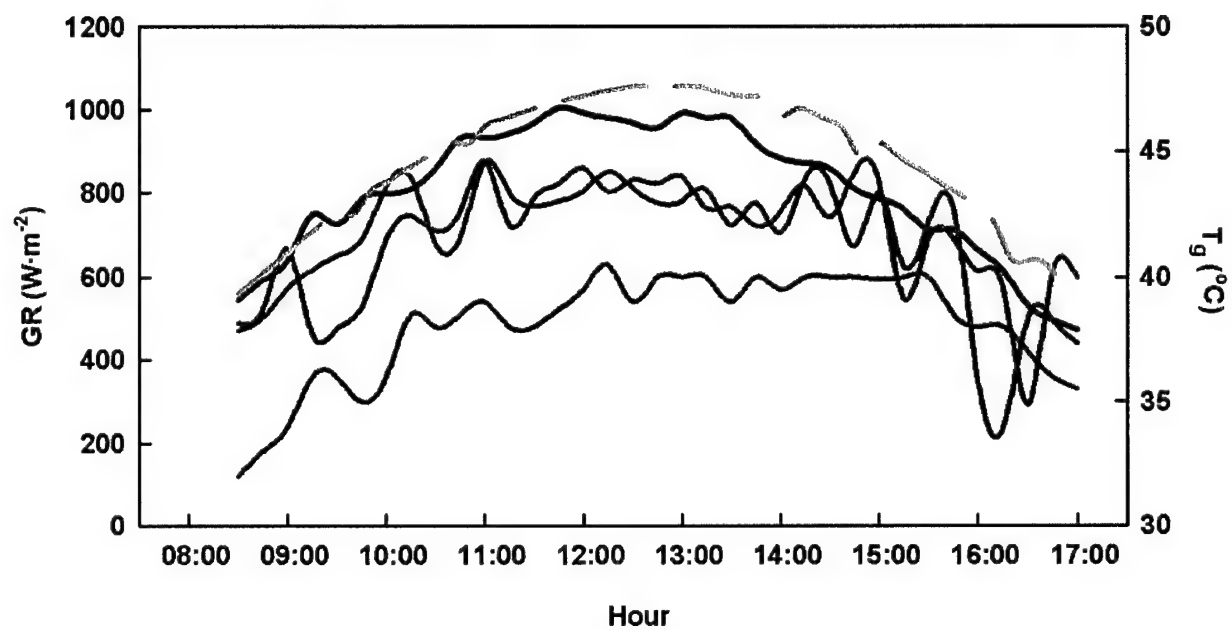
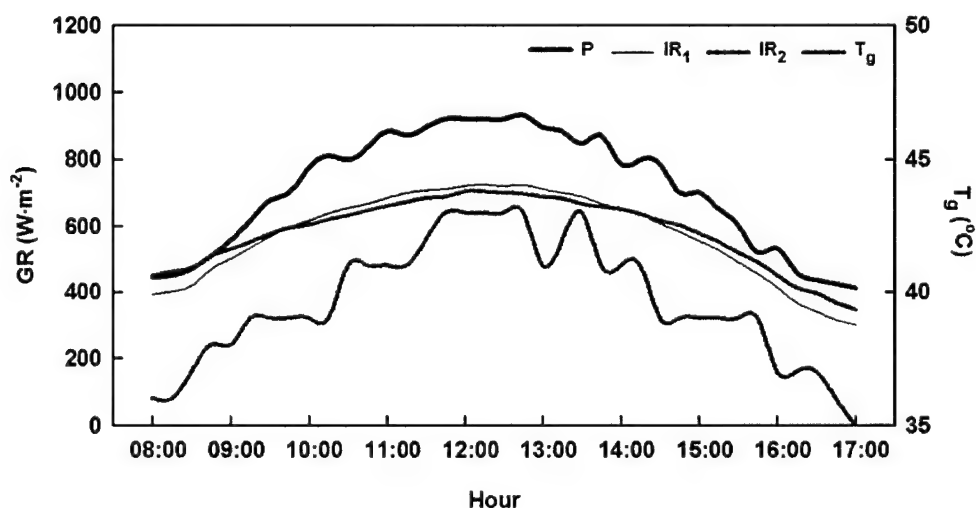


Figure 24: Global radiation (GR) measured by 2 pyranometers (P, P_{IMS}), 2 infra-red (IR) light sensors and black globe thermometer (T_g) at 900 m from sea level.



The ESI was calculated separately using the three IR sensors (ESI_{IR1} , ESI_{IR2} , ESI_{IR3}) and the pyranometer (ESI_P) measurements, and applied separately to each of the 6 locations differing in their distances below (-200 m and -400 m) or above sea level (Figures 26-31). No significant differences were found between the 3 different ESIs calculated with IR sensor or the pyranometer and the WBGT, as depicted in Table 3,

Figure 25: Global radiation (GR) measured by pyranometer (P), 2 infra-red (IR) light sensors and black globe thermometer (T_g) at 1600 m from sea level.



and for each of the locations in Appendix C. However, when the ESI was compared to the WBGT index, no significant differences were found in 4 locations (-400 m below and 30 m, 400 m and 900 m above sea level). At -200m below sea level, WBGT was significantly lower ($P < 0.05$) than ESI, and at 1600m above sea level, WBGT values were significantly higher ($P < 0.05$) than the ESI values.

Table 3. Mean (\pm SD) and range of the modified ESI and the WBGT index calculated from global radiation measured by pyranometer (ESI_P) and 3 different IRL sensors (ESI_{IR}). Database was collected from 6 different meteorological stations at different heights below and above sea level (n=238).

	ESI_P	ESI_{IR1}	ESI_{IR2}	ESI_{IR3}	WBGT($^{\circ}$ C)
Mean \pm SD	26.03 \pm 3.11	26.31 \pm 3.00	26.50 \pm 2.88	27.21 \pm 2.76	26.39 \pm 2.63
Range	18.68-32.63	19.28-32.21	19.79-32.29	20.61-32.33	18.37-30.76

Figure 26: Comparison of the modified ESI with the WBGT index. ESI was calculated from global radiation (GR) measured by pyranometer (ESI_p) and 3 different IR light sensors (ESI_{IR}) at -400 m below sea level.

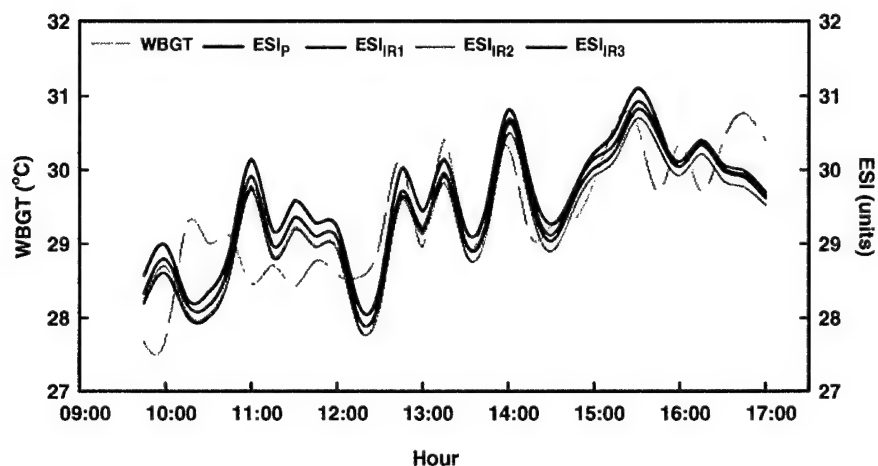


Figure 27: Comparison of the modified ESI with the WBGT index. ESI was calculated from GR measured by pyranometer (ESI_p) and 3 different IR light sensors (ESI_{IR}) at -200 m below sea level.

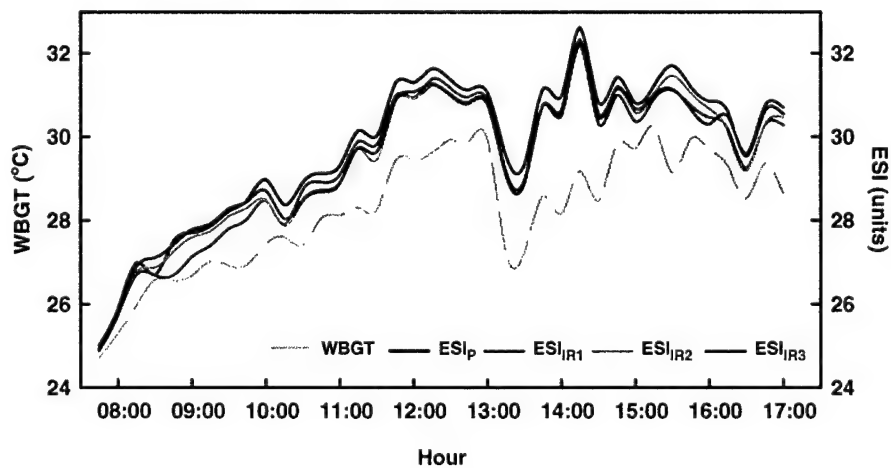


Figure 28: Comparison of the modified ESI with the WBGT index. ESI was calculated from GR measured by pyranometer (ESI_p) and 3 different IR light sensors (ESI_{IR}) at 30 m from sea level.

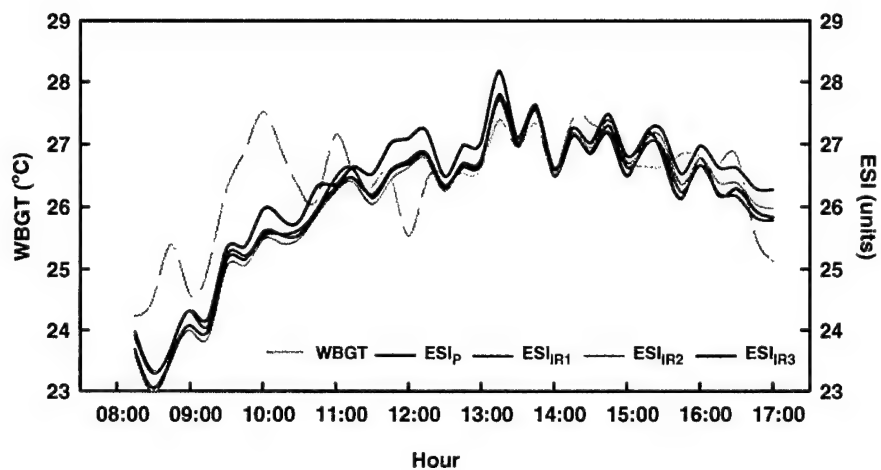


Figure 29: Comparison of the modified ESI with the WBGT index. ESI was calculated from GR measured by pyranometer (ESI_p) and IR light sensors (ESI_{IR}) at 400 m from sea level.

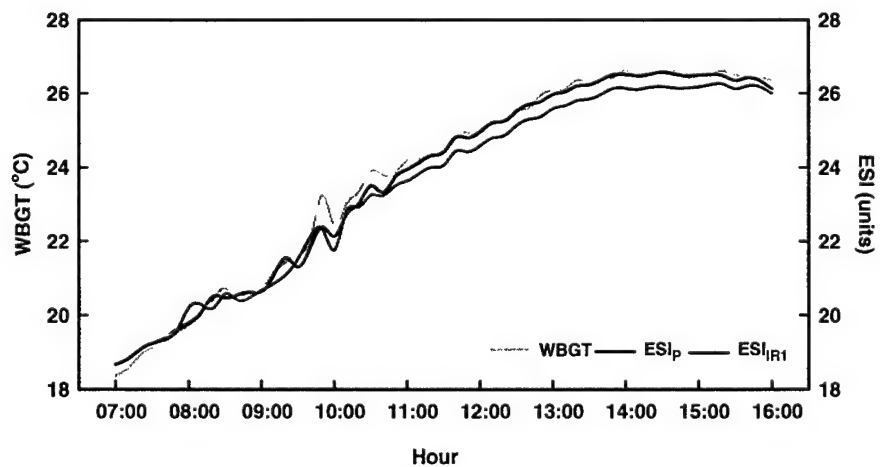


Figure 30: Comparison of the modified ESI with the WBGT index. ESI was calculated from GR measured by pyranometer (ESI_p) and 2 different IR light sensors (ESI_{IR}) at 900 m from sea level.

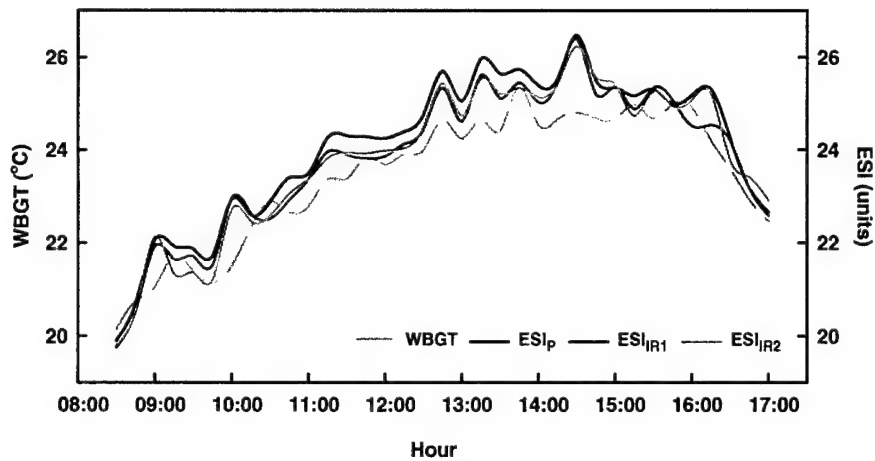
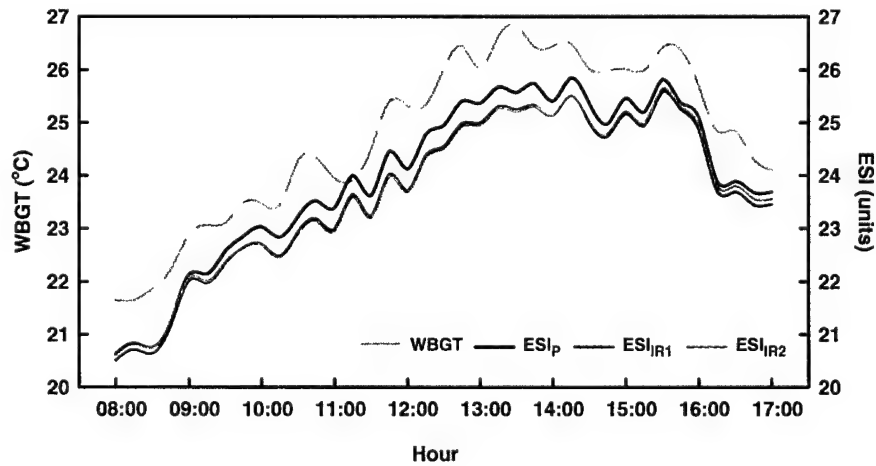


Figure 31: Comparison of the modified ESI with the WBGT index. ESI was calculated from GR measured by pyranometer (ESI_p) and 2 different IR light sensors (ESI_{IR}) at 1600 m from sea level.



DISCUSSION

STUDY I

The modified ESI introduced in this study to evaluate environmental heat stress reliably matches values calculated by using the conventional WBGT. This modified ESI is based on the same parameters as ESI (T_a , RH and SR), which integrates the thermal load derived by the specific climatic conditions. However, separate analysis of the 19 different databases obtained from the 19 different locations revealed changes in the ESI constants of the variables, interaction, and transformation. Arithmetically, the first developed ESI was well correlated to WBGT (16). However, validation of the modified ESI for these large databases further improved the correlation with the WBGT ($(R^2 \geq 0.898)$). The strength of any prediction index is its ability to predict with high correlation the measured or calculated universal index under widely varied climatic conditions.

ESI differs from other indices that have been suggested in the past in two critical ways. First, this stress index for the first time uses direct measurements of SR and RH. These direct measurements of RH and SR, when used in ESI, are not as cumbersome as measuring T_g and T_w for calculating the WBGT. Second, the three meteorological variables used in ESI are characterized by fast-reading responses that take only a few seconds to reach equilibrium. For an index to be valid and practical, it should allow the comparison and evaluation of a combination of different meteorological parameters as far as their influence on the individual is concerned. It also helps to find different combinations of these parameters that cause equal subjective heat sensations. Moreover, the index must enable one to assess the different weights of each of the meteorological parameters on the individual (6).

In conclusion, this study separately confirms the results of a previous study (16), which initially introduced ESI and found a high correlation with WBGT. However, in the present study, ESI was evaluated using a larger database with revised constants included in its determination and a higher correlation with WBGT. Therefore, the ESI has the potential to serve as a substitute to the WBGT index and to be used for safety limits during training and military activity. It can also serve as a part of the guidelines for work rest cycles and fluid replacement. To implement the current guidelines and limitations for exercise in a hot climate, there is a great need for the development of an accurate, portable heat stress measurement device. This study suggests that the ESI is an ideal index to be used in such a device. However, further evaluation of ESI is required for validation with specific physiological variables (e.g., sweating rate, heart rate, and internal body temperatures).

STUDY II

In a previous study (16), a newly developed algorithm from light sensor appeared valid for use in determining predictive global radiation (PGR), since the correlation coefficient between PGR and measured global radiation by pyranometer was very high. In this study, we additionally evaluated PGR at different heights below and above sea level, and the database for this study was collected at 6 separate locations. The range of the measurements for each day was wide as seen in Table 2. Analyses of the global radiation measurements at different heights above and below sea level is limited in this study because a real comparison can be done only from a large database containing annual GR measurements collected at the same time at the 6 locations. In an analysis made at different heights from sea level, which were made by the IMS over 26 years, it was found that at -208 m below sea level, GR values were lower by $100 \text{ W}\cdot\text{m}^{-2}$ from measurements at 815 m above sea level. These differences are consistent, but vary according to the month of the year. However, mean GR values were higher at -395m than at -208m. The latter might be explained by other factors that influence the GR apart from the topographical height from sea level (e.g., cloudiness, atmospheric transparency, and reflective radiation).

In analyzing the data from the 3 IR light sensors and the pyranometer, we can draw two conclusions. First, there were no significant differences between these 3 sensors, which strengthens the reliability and validity of the IR light sensor to measure GR. The second conclusion relates to a comparison between the P measurements and the IR light sensors. Higher values for P were measured in all the 6 locations. Although differences were not significant for all the locations, for better accuracy, refinement of the model that predicts global radiation (PGR) from the IR light sensor should be considered.

In this study, ESI was applied by using 3 different IR light sensors and pyranometer measurements for global radiation. However, no statistically significant differences were found between the ESI calculated with either sensor (Figures 26-31). Overall, when WBGT was applied to the same 6 databases, no statistically significant differences were found in 4 databases between ESI and WBGT. However, at -200 m below sea level, WBGT values were significantly lower ($P < 0.05$) than ESI, and at 1600 m above sea level, WBGT values were higher than ESI.

The present study derived a simple fast response method to measure and evaluate global radiation. This method is easier to measure, interpret, and use as a potential substitute for T_g , which is incorporated in the WBGT.

CONCLUSIONS

Although the WBGT is the most common heat stress index and has been adopted by many organizations, we introduced and evaluated in this study a new environmental stress index (ESI) that may be a reasonable substitute for the conventional index. The ESI was fabricated using new micro-sensors that measure climatic conditions with programmable microchips. The present study confirms that the simple ESI is valid to evaluate wide climatic conditions. This simple index should be easier to measure since it is based on more commonly used sensors (e.g., RH, GR) than the WBGT index. The ESI is capable of overcoming the technical difficulties of measuring WBGT (e.g., T_g , T_w), while providing an easy to operate index based on fast response micro-sensors to assess heat stress. This development is very encouraging since there already exist micro-sensors for measuring T_a and relative humidity (RH) that are available off-the-shelf. We suggest that ESI has the potential to be widely accepted, used universally, and easily implemented in a relatively small portable device. However, further investigation is necessary in order to refine the PGR distinct from the IR-light sensor.

REFERENCES

1. American College of Sports Medicine. Position stand on heat and cold illnesses during distance running. *Med. Sci. Sports Exerc.* 28(12): i-x, 1996.
2. Bedford T. The warmth factor in comfort at work: a physiological study of heating and ventilation. Industrial Health Research Board 76. HMSO London 1936; In: *Indoor Climate*, edited by D. A. McIntyre. London: Applied Science, 1980, p. 161-196.
3. Burr, R. E., *Heat illness: a handbook for medical officers*. Natick, MA: USARIEM. Technical Report T91-3, 1991.
4. Chaurel, C., M. Mercier-Gallay, M. Stoklov, S. Romazini, and A. Perdrix. Environmental stresses and strains in an extreme situation: the repair of electrometallurgy furnaces. *Int. Arch. Occup. Environ. Health.* 65: 253-258, 1993.
5. Froom, P. E. Krisal-Boneh, J. Ribak, and Y.G. Caine. Predicting increases in skin temperature using heat stress indices and relative humidity in helicopter pilots. *Isr. J. Med. Sci.* 28: 608-610, 1992.
6. Givoni, B., and R.F. Goldman. Predicting rectal temperature response to work environment and clothing. *J.Appl. Physiol.* 32: 812-822, 1972.
7. Gonzalez, R.R., G.N. Sexton, and K.B. Pandolf. US-2, Biophysical evaluation of the wet globe temperature index (Botsball) at high air movements and constant dew point temperature. In: *14th Commonwealth Defence Conference on Operational Clothing and Combat Equipment*, edited by G.Tilley. Melbourne: Commonwealth Press, 1985, p 1-20.
8. Gun, R.T., and G.M. Budd. Effects of thermal, personal and behavioral factors on the physiological strain, thermal comfort and productivity of Australian shearers in hot weather. *Ergonomics* 38: 1368-1384, 1995.
9. Haldane, J.C. The influence of high temperature. *J. Hyg.* 5: 404-409, 1905.
10. Hill, L., C.W. Griffith, and M. Flack. The measurement of the rate of heat loss at body temperature by convection, radiation and evaporation. *Phil Trans Bull.* 207: 183, 1916.
11. Majumdar, N.C. Indices of heat stress. In: *Heat Stress, edited by B. Bhatia and C.K. Varshneey*. New Delhi: Interprint, 1978, p. 11-75.
12. Matthew, W.T., G. J. Thomas, L.E. Armstrong, P.C. Szlyk, I.V. Sils, and R.W. Hubbard. (WGT) performance characteristics and their impact on the implementation of military hot weather doctrine. Natick, MA: USARIEM. Technical Report T9-86, 1986.

13. McCann, D.J., and W.C. Adams. Wet bulb globe temperature index and performance in competitive distance runners. *Med. Sci. Sports Exerc.* 27: 955-961, 1997.
14. Montain, S.J., W.A. Latzka, and M.N. Sawka. Fluid replacement recommendations for training in hot weather. *Mil. Med.* 164: 502-508, 1999.
15. Moran, D.S., and K.B. Pandolf. Wet Bulb Globe Temperature (WBGT) – to what extent is GT essential? *Aviat. Space Environ. Med.* 70: 480-484, 1999.
16. Moran, D.S., K.B. Pandolf, Y. Shapiro, A. Frank, Y. Heled, Y. Shani, W.T. Matthew, and R.R. Gonzalez. The role of global radiation measured by a light sensor on heat stress assessment. *J. Therm. Biol.* 26:433-436, 2001.
17. Moran, D.S., K.B. Pandolf, Y. Shapiro, Y. Heled, Y. Shani, W.T. Matthew, and R.R. Gonzalez. An environmental stress index (ESI) as a substitute for the wet bulb globe temperature (WBGT). *J. Therm. Biol.* 26:427-431, 2001.
18. National Institute for Occupational Safety and Health. Occupational exposure to hot environments. Washington, D.C.: Department of Health and Human Services. Report DHHS86-113, 1986.
19. Ralston, M.L., and R.L. Jennrich. DUD-a derivative free algorithm for nonlinear least squares. *Technometrics* 20: 7-14, 1978.
20. Singh, A.P., D. Majumdar, M.R. Bhatia, K.K. Srivastava, and W. Selvamurthy. Environmental impact on crew of armoured vehicles: effects of 24 h combat exercise in hot desert. *Int.J. Biometeorol.* 39: 64-66, 1995.
21. Sohar, E., C.H. Birenfeld, Y. Shoenfeld, and Y. Shapiro. Description and forecast of summer climate in physiologically significant terms. *Int. J. Biometeor.* 22: 75-81, 1978.
22. Sohar, E., J. Tennenbaum, and N. Robinson. A comparison of the cumulative discomfort index (Cum. DI) and the cumulative effective temperature (Cum. ET) as obtained by meteorological data. In: *Biometeorology*, edited by S.W. Tromp. Oxford: Pergamon Press, 1962, p. 395-420.
23. Tennenbaum, J., E. Sohar, R. Adar, T. Gilat, and D. Yaski, D. The physiological significance of the cumulative Discomfort Index. *Harefuah* 60: 315-319, 1960.
24. Thom, E.C. Discomfort index. *Weatherwise* 12: 57, 1959.
25. Vernon, H. The measurement of radiant heat in relation to human comfort. *J. Indust. Hyg.* 14: 95-111, 1932.

26. Yaglou, C.P. Temperature, humidity and air movement in industries. *J. Indust. Hyg.* 9: 297, 1927.

27. Yaglou, C.P., D. Minard. Control of heat casualties at military training centers. *Arch. Ind. Hlth.* 16: 302-305, 1957.

**APPENDIX A. Mean (\pm SD) and range of environmental measurements of the ESI
validation versus WBGT at the 19 different locations**

	T_a (°C)	T_w (°C)	RH (%)	T_g (°C)	SR (W·m ⁻²)	WBGT (°C)
Station no. 1	19.29 \pm 5.75 8.10-34.80	3.36 \pm 2.51 6.30-21.80	53 \pm 25 6-98	22.12 \pm 10.23 5.00-50.00	277 \pm 352 0-1172	15.71 \pm 3.96 6.87-26.21
Station no. 2	20.33 \pm 4.84 8.90-39.20	15.95 \pm 2.48 7.90-22.60	65 \pm 19 5-67	25.48 \pm 9.08 8.07-50.01	240 \pm 308 0-993	18.30 \pm 3.70 8.15-27.94
Station no. 3	19.35 \pm 5.29 9.50-40.60	15.32 \pm 2.20 9.10-22.00	68 \pm 23 9-100	22.24 \pm 9.97 6.40-49.20	231 \pm 296 0-972	17.11 \pm 3.75 8.69-27.88
Station no. 4	26.00 \pm 4.73 15.40-39.00	16.28 \pm 2.00 10.40-21.50	35 \pm 16 5-92	28.29 \pm 8.71 8.70-53.20	280 \pm 354 0-1107	19.65 \pm 3.14 10.88-28.00
Station no. 5	19.95 \pm 5.97 5.30-37.80	15.37 \pm 3.30 4.90-29.70	64 \pm 24 10-100	19.76 \pm 10.97 5.10-45.70	259 \pm 325 0-1143	16.71 \pm 4.67 4.28-31.67
Station no. 6	25.20 \pm 5.21 14.20-38.60	16.41 \pm 2.10 8.40-22.70	39 \pm 17 5-95	30.09 \pm 10.58 11.86-59.42	247 \pm 314 0-989	20.02 \pm 3.63 10.03-30.26
Station no. 7	17.76 \pm 5.22 9.30-32.40	11.79 \pm 2.28 5.40-19.70	50 \pm 26 5-97	21.83 \pm 9.94 5.86-50.70	282 \pm 363 0-1337	14.40 \pm 3.59 6.31-25.88
Station no. 8	15.38 \pm 5.75 0.80-33.20	12.23 \pm 3.49 0.60-22.60	72 \pm 23 26-100	17.60 \pm 9.51 0-47.10	270 \pm 343 0-1152	13.62 \pm 4.73 0.70-28.28
Station no. 9	27.59 \pm 3.96 18.40-38.80	18.39 \pm 1.81 12.30-25.40	39 \pm 11 10-99	33.64 \pm 8.27 12.56-59.33	266 \pm 338 0-1089	22.36 \pm 2.80 14.66-29.84
Station no. 10	20.83 \pm 5.61 9.20-37.00	15.80 \pm 2.89 8.00-24.00	61 \pm 20 14-94	23.93 \pm 10.56 5.92-52.80	262 \pm 331 0-1131	17.93 \pm 4.37 7.81-30.30
Station no. 11	21.05 \pm 4.12 13.90-36.40	16.48 \pm 1.95 10.30-23.00	64 \pm 20 14-95	20.69 \pm 10.18 10.90-54.20	277 \pm 338 0-1055	17.78 \pm 3.34 9.27-29.73
Station no. 12	24.37 \pm 5.89 13.70-37.70	17.53 \pm 1.77 12.00-25.10	54 \pm 26 10-97	28.18 \pm 11.11 11.20-56.10	334 \pm 385 0-1063	20.34 \pm 3.65 12.35-29.54
Station no. 13	24.99 \pm 3.61 15.10-33.30	20.78 \pm 1.96 13.90-24.80	68 \pm 15 27-97	31.23 \pm 8.65 14.50-46.60	312 \pm 367 0-1098	23.29 \pm 3.14 14.22-29.19
Station no. 14	24.35 \pm 4.37 14.90-34.60	20.50 \pm 1.91 13.70-25.70	72 \pm 20 25-100	28.58 \pm 10.56 12.50-50.40	305 \pm 355 0-1073	22.51 \pm 3.53 13.58-30.45
Station no. 15	32.64 \pm 4.75 20.80-44.30	19.51 \pm 1.46 15.50-25.00	27 \pm 13 2-68	35.93 \pm 8.26 19.00-55.00	328 \pm 379 0-1038	24.11 \pm 2.72 16.94-30.69
Station no. 16	25.88 \pm 5.09 13.90-40.80	20.36 \pm 2.21 10.80-25.60	62 \pm 20 10-100	25.53 \pm 10.69 5.20-52.70	324 \pm 367 0-1022	21.95 \pm 3.77 10.07-30.54

Station no. 17	23.48±4.49 13.90-36.30	15.75±2.15 9.10-22.30	44±22 2-96	28.61±10.03 12.00-54.70	349±403 0-1147	19.09±3.38 11.84-29.03
Station no. 18	26.38±4.65 15.50-41.60	21.03±2.40 12.60-27.80	63±19 17-94	29.99±9.84 12.10-56.60	320±367 0-1038	23.36±3.69 13.16-32.58
Station no. 19	24.00±2.67 18.10-33.40	19.76±1.99 12.20-25.10	67±17 16-95	24.90±9.74 9.00-46.50	318±366 0-1034	21.21±2.94 13.81-29.59

APPENDIX B. Mean (\pm SD) and range of global radiation (GR) measured using 2 pyranometers [by Heller Institute (P) and by Israeli Meteorological Service (P_{IMS})], black globe thermometer (T_g), and 3 infra-red (IR) light sensors. Database was collected from 6 different meteorological stations at different distances (Dist.) above and below sea level.

Dist. from Sl (m)	P ($W \cdot m^{-2}$)	P_{IMS} ($W \cdot m^{-2}$)	T_g ($^{\circ}C$)	IR_1 ($W \cdot m^{-2}$)	IR_2 ($W \cdot m^{-2}$)	IR_3 ($W \cdot m^{-2}$)	T_a ($^{\circ}C$)	T_w ($^{\circ}C$)
-400	817 \pm 180 387- 1028	917 \pm 77 722-992	49.20 \pm 1.52 45-52	721 \pm 127 410-849	672 \pm 152 325-828	735 \pm 152 370-887	35.75 \pm 2.05 32.20- 38.60	22.82 \pm 0.85 22.00- 24.50
-200	748 \pm 214 205-967	-----	40.71 \pm 4.45 30-48	581 \pm 204 151-821	637 \pm 161 160-814	674 \pm 150 179-844	31.99 \pm 2.99 26.10- 36.40	24.17 \pm 0.96 22.50- 26.00
30	707 \pm 183 290- 1028	810 \pm 187 368-990	40.11 \pm 2.01 35-45	645 \pm 165 296-819	628 \pm 181 192-840	683 \pm 179 220-871	27.47 \pm 1.12 24.20- 28.90	22.31 \pm 0.72 21.00- 23.00
400	-----	709 \pm 348 40-1053	-----	688 \pm 155 237-875	694 \pm 139 292-876	-----	26.11 \pm 4.16 19.10- 31.10	20.68 \pm 1.42 18.20- 22.50
900	806 \pm 159 471- 1003	913 \pm 153 560- 4058	38.03 \pm 2.20 32-40.50	-----	-----	-----	24.94 \pm 1.56 21.90- 27.90	19.03 \pm 1.31 16.50- 21.00
1600	708 \pm 177 411-931	-----	45.07 \pm 2.63 39-48.50	-----	572 \pm 133 301-724	579 \pm 105 346-704	27.50 \pm 0.86 25.50- 28.90	20.11 \pm 1.84 17.00- 22.50

APPENDIX C. Mean (\pm SD) and range of the modified ESI and the WBGT index calculated from global radiation measured by pyranometer (ESI_P) and 3 different infra-red light sensors (ESI_{IR}). Database was collected from 6 different meteorological stations at different distances (Dist.) above and below sea level.

Dist. from SL (m)	ESI_P	ESI_{IR1}	ESI_{IR2}	ESI_{IR3}	WBGT (°C)
-400	29.59 \pm 0.77 29.19-31.10	29.40 \pm 0.86 27.89-30.93	29.30 \pm 0.77 27.90-30.70	29.42 \pm 0.77 28.02-30.83	29.39 \pm 0.86 27.67-30.76
-200	29.60 \pm 1.69 25.01-32.63	29.26 \pm 1.67 24.90-32.21	29.38 \pm 1.61 24.92-32.29	29.45 \pm 1.57 24.96-32.33	28.26 \pm 1.32 24.71-30.25
30	26.21 \pm 1.12 23.32-28.18	26.09 \pm 1.08 23.31-27.74	26.05 \pm 1.19 22.99-27.76	26.16 \pm 1.19 23.07-27.81	26.38 \pm 0.85 24.23-27.52
400	23.78 \pm 2.71 18.37-26.60	23.71 \pm 2.68 18.68-26.57	-----	-----	23.78 \pm 2.71 18.37-26.60
900	24.06 \pm 1.62 19.90-26.47	23.82 \pm 1.58 19.75-26.40	23.83 \pm 1.63 19.79-26.24	-----	23.42 \pm 1.43 20.14-25.36
1600	23.96 \pm 1.55 20.63-25.85	-----	23.69 \pm 1.49 20.51-25.59	23.70 \pm 1.47 20.61-25.65	27.07 \pm 1.60 24.23-30.29